Engineering & Technology in India

www.engineeringandtechnologyinindia.com

Strength for Today and Bright Hope for Tomorrow

ISSN 2472-8640

Volume 1:3 April 2016

Contents

Dare to Give!

A Call from Philosopher, Educationist and Entrepreneur

Jimmy Teo

Some 41 years ago, I was having dinner alone at Potong Pasir (Pek Suan Phu) at Tanjung Pinang, Bintang Island, Riau Archipelago, Indonesia.

My eyes got a little cloudy when recollecting that moment.

I need to share for posterity sake:

1 I love seafood. Rarely, I eat alone. For whatever reason, that evening, I was there alone. It was also my 1st time eating at this large alfresco food place where the locals frequent – brightly lighted by kerosene lamps & fronted by lots of 'push carts' hawkers.

2 I ordered steamed shell fish. And when I was waiting for my dish to arrive, I was enthralled by an interesting incident. A thin man, followed by his wife & 3 children were marching, all in a single file to a table about 50 meters away from me. It was quite spectacular in that, they were marching, not walking leisurely. From their clothes, one can see that they were very poor & very thin. Why they were there to eat was a wonder to me. I guess then that the man of the house decided to give the whole family a treat despite their poverty or that they freshly arrived from the jungles (Pulau Bintang was then not developed, with lots of jungle hinterland).

3 I saw them got seated & ordered something from the enquiring hawkers.

4 I then asked the hawker serving me to do me a favour. I told him to please tell the other hawker serving that family not to accept any payment. I will pay for all that they consume that evening. And he quickly went over to tell his hawker friend that I will pick up the bill for that family.

5 As I was eating my dish, to my surprise, the whole same family came to me (again in single file) to thank me. I was caught by surprise. They ate so fast & probably so

simply, as I guess they could not afford more. I think I must have paid only a few Singapore dollars for their whole family. And they came to thank me! They could not believe that there are people in this world willing to do that!

My little action touched the life of the hawker who sold me my food as he was also very touched; and also his hawker friend who provided the food & was paid by me.

Then, the family who ate the food who could not help but be thankful & grateful.

And now, all of you who read this article may be touched as well.

Only a few dollars (or a few Indian rupees), and it helped make the world a better place.

May we dare to be generous;
To give to the needy
Showing the way for others
To do likewise.

May we infuse this world
With kindness & goodness
By our thoughts, actions, smiles
And our words.

8.32am/Thurs/3.12.15

===

Jimmy Teo
Singapore
teojimmy07@gmail.com

==
Engineering & Technology in India www.engineeringandtechnologyinindia.com
Vol. 1:3 April 2016
==

Triple Adjacent Error Correction (TAEC) Code for Data Bits in Memory Chips

Ayyappan S., M.E.
Srividhya B., M.E. Student
==

Abstract

In this paper, a new double-adjacent-error- correction and triple -adjacent-error -correction (DAEC- TAEC) code is proposed for simultaneous testing of the most general memory fault models in data bit arrays of memories. Simultaneous testing of data bit and check bit arrays eliminates the test time and hardware overheads and also reduces the complexity. In order to test data bit and check bit arrays simultaneously, the pro-posed DAEC-TAEC code generates the identical data background patterns for data bit and check bit arrays. The testable faults using the proposed DAEC-TAEC code are the most general memory fault models such as single-cell faults and interword and intraword coupling faults. Simultaneous testing of data bit and check bit arrays using the proposed SEC-DAEC codes brings significant decreases in the time required for memory array tests for 16, 32, and 64 data bits per word.

Key words: Error correction code, fault model, memory test, word-oriented memory.

I. INTRODUCTION

Transient errors are caused by cosmic neutrons, alpha particles, and radiations and have emerged as a key reliability concern in semiconductor memories .Error correction code (ECC) techniques have been widely used to correct transient errors and improve the reliability of memories. ECC words in memories consist of data bits and additional check bits because the ECCs used in memories are typically from a class of linear block codes. During the write operations of memories, data bits are written in data bit arrays, and check bits are concurrently produced using the data bits and stored in check bit arrays. The check bit arrays, just like the data bit arrays, should be tested prudently for the same fault models if reliable error correction is to be insured. However, it is not feasible to directly access check bit arrays from outside the chip, and additional test time and hardware overheads are often unavoidable for check bit screening [4], [5]. Also, memory test cost increases due to the additional test time for the check bit array and hardware overheads.

Simultaneous testing of data bit and check bit arrays has been proposed in order to reduce the test time and hardware overheads required for separate check bit array tests . SEC code has been presented in order to test various memory fault models in both data bit and check bit arrays simultaneously in our previous work.

In this paper, the double-adjacent-error-correction and the triple -adjacent - error-correction (DAEC-TAEC) code without the DED function will be considered to test the most general fault models in data bit and check bit arrays simultaneously. Simultaneous testing of data bit and check bit arrays can reduce the additional test time and hardware overheads required for separate check bit array tests. In addition, the number of ones (1's) in the H-matrix of the proposed SEC-DAEC code can be made to be close to the theoretical minimum number. Also, the proposed DAEC-TAEC code can be used in conjunction with bit interleaving such as the DAEC-TAED-TAEC codes.

In this paper double-adjacent-error-correction and triple- adjacent-error correction (DAEC-TAEC) code without the DED function will be considered to test the most general fault models in data bit and check bit arrays simultaneously. Simultaneous testing of data bit and check bit arrays can reduce the additional test time and hardware overheads required for separate check bit array tests. The required number of check bits for the DAEC-TAEC codes is the same as those for the SEC-DED. In addition, the number of ones (1's) in the H-matrix of the proposed DAEC-TAEC code can be made to be close to the theoretical minimum number. Also, the proposed DAEC-TAEC code can be used in conjunction with bit interleaving such as the DAEC-TED-TAEC codes.

II. METHOD FOR SIMULTANEOUS TESTING

In order to test data bit and check bit arrays simultaneously for the same fault model, the data patterns and the read and write operation sequence for the tests should be identical for the data bit and check bit arrays. In addition, the test responses for check bit arrays should be evaluated together with data bit arrays. Because the identical data background (DB) patterns cannot be generated using just any ECC ,an appropriate ECC is required in order to generate identical DB patterns for data bit and check bit arrays. If certain regularity can be found in DBs for data bit arrays, the identical DB patterns for data bit and check bit arrays can be generated to conform to that regularity. The DB patterns for various fault models in word-oriented memories (WOMs) have previously been suggested .DBs having the same regularity can test single-cell faults and interword coupling faults (CFs) because any DB is acceptable for single-cell faults and interword CFs .

Fig. 1 shows the block diagram of the ECC processing circuit for simultaneous testing. The ECC processing circuit generally consists of the following four units: 1) a check bit generator, 2) a syndrome generator, 3) an error locator, and 4) a corrector .In order to detect occurrences of errors, an error detector is additionally required. It is assumed that the identical DB patterns for data bit and check bit arrays are already generated using the check bit generator based on the appropriate ECC. In order to evaluate the occurrences of errors, two test responses are used. The first test response is the corrected DB in which errors are corrected by the ECC techniques. The second test response is the error detection signal which indicates the existence of errors regardless of the number of erroneous bits and is the OR-sum of the syndromes

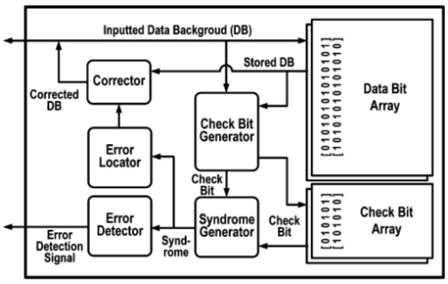

Fig.1 Block diagram of the ECC processing circuit for simultaneous testing

The error detection signal and corrected DB according to the number of erroneous bits. For the cases of no error, a single bit error, or an adjacent double bit error in the ECC word, the corrected DB is identical for the inputted DB when the DAEC-TAEC code is used. However, the corrected DB is not identical for the inputted DB when a non-adjacent double or more bit error occurs in the ECC word. When there is no error in the ECC word, the syndromes become zero vectors and the error detection signal becomes zero. When a single or double bit error occurs in the ECC word, the syndromes become non-zero vectors and the error detection signal becomes one. However, some syndromes generated by triple or more bit errors in the ECC word can be a zero vector and the error detection signal becomes zero.

Consequently, it is unknown whether the error detection signal becomes zero or one when triple or more bit errors occur in the ECC word. The occurrences of errors in the data bit and check bit arrays can be evaluated using a combination of the error detection signal and corrected DB. If the error detection signal is zero and the corrected DB is the same as the inputted DB, there is no error. If the error detection signal is one or the corrected DB is not the same as the inputted DB, there is an error in the ECC word. Therefore, simultaneous testing of data bit and check bit arrays can be realized without the test time and hardware overheads required for separate check bit array tests if the appropriate ECC is constructed to generate identical DB patterns for data bit and check bit arrays.

III. BINARY LINEAR BLOCK CODES

The SEC codes, SEC-DED codes, SEC-DED-DAEC codes, and SEC-DAEC codes are binary linear block codes. A binary (n, k) linear block code is a k-dimensional subspace of a binary n-dimensional vector space. An n-bit ECC word consists of $n - r$ data bits and r check bits. A binary (n, k) systematic linear block code is represented as a $r \times n$ H-matrix consisted of a $r \times k$ matrix for the data bits and a $r \times r$ identity matrix for the check bits. The H-matrices of the conventional DAEC-TAEC codes are constructed under the following four common constraints:

1) There should be no zero-weight columns.
2) Each column should be different from any other column.
3) Each exclusive-or-sum (xor-sum) of any two columns should be different from any column in the H-matrix.
4) Each xor-sum of two adjacent columns should be different from any of the columns and the xor-sums of two adjacent columns.

The first and second constraints are related with the single- error-correction (SEC) function. The first constraint guarantees the syndrome to be a non-zero vector when a single bit error occurs. The second constraint ensures that all single bit errors are correctable. The third constraint is related with the DED function. In the odd-weight-column code which is the most widely used SEC-DED code in memories, the XOR-sum of any two odd- weight columns always becomes an even-weight vector and then the third constraint is satisfied. When the odd-weight-column code is used, if the weight of the syndrome is an even number, a double bit error is deemed to be detected. In the conventional SEC-DED- DAEC codes, not only odd-weight columns but also even-weight columns satisfying the third constraint are used. If the syndrome is a non-zero vector and does not match any column in the H-matrix, a double bit error is deemed to be detected. The fourth constraint guarantees that all adjacent double bit errors are correctable.

In order to construct the conventional SEC codes enabling simultaneous testing of the data bit and check bit arrays in the previous work, the following essential constraint for simultaneous testing is required:

In each row of the H-matrix excluding the identity matrix, the number of 1's in column-indexed positions that are such that the remainder in the division of j by q ($j \bmod q$) is the same as $i \bmod q$ should be an odd number, where i and j denote the row and column indices, respectively. Otherwise, the number of 1's in each of the groups formed by the column-indexed positions that have the same value of $j \bmod q$ (but different from the value of $i \bmod q$) should be an even number. For the conventional SEC code, q is four when r is four or five. When r is larger than or equal to six, q is the smallest power of two larger than or equal to r.

By the essential constraint for simultaneous testing, the r check bits ($c0 \ldots cr-1$) should have the same values of the r lower data bits ($d0 \ldots dr-1$) when a q-bit sequence is repeated in DBs.

However, it is difficult to construct the DAEC-TAEC codes enabling simultaneous testing of data bit and check bit arrays because the essential constraint for simultaneous testing is not met for the third constraint of the DAEC-TAEC codes regarding the DED function. In order to satisfy the essential constraint for simultaneous testing, numerous even weight columns should be required in the H-matrix. However, the third constraint of the SEC-DED-DAEC codes regarding the DED function makes the number of even-weight columns equal to zero in the odd-weight-column code, or very small in the conventional SEC-DED-DAEC codes. The DED function is ineffective in many types of memory when used together with the DAEC function because it is impossible to distinguish adjacent double bit errors from non-adjacent double bit errors. In this paper, the proposed SEC-DAEC code will be constructed without the aforementioned third constraint for the conventional SEC-DED-DAEC codes in order to increase the number of even-weight columns. Consequently, the essential constraint required for simultaneous testing can be satisfied.

IV. PROPOSED SEC-DAEC CODE FOR SIMULTANEOUS TESTING

A new DAEC-TAEC code is proposed in order to satisfy the essential constraint for simultaneous testing. The proposed SEC- DAEC code enables to test single-cell faults, interword CFs and intraword CFs in both data bit and check bit arrays simultaneously. A simple pattern having a cell count of some power of two is repeated in its sequence in DBs used for WOM tests The H-matrix of the proposed DAEC-TAEC code is constructed using this regularity in DBs. The identical DB patterns for data bit and check bit arrays can be generated using the proposed DAEC-TAEC code. In addition, the proposed DAEC-TAEC code is constructed in order to reduce the number of 1's in the H-matrix. The H-matrix of the $(2^{r-2} + r, 2^{r-2})$ proposed SEC-DAEC code consists of 2^{r-2} data bits and r check bits and is subject to the following seven constraints:

1) There should be no zero-weight columns.
2) Each column should be different from any other column.
3) Each xor-sum of two adjacent columns should be different from any of the columns and the xor-sums of two adjacent columns.
4) In each row of the H-matrix excluding the identity matrix, the number of 1's in column-indexed positions that are such that $j \bmod q$ is the same as $i \bmod q$ should be an odd number, where i and j denote the row and column indices, respectively. Otherwise, the number of 1's in each of the groups formed by the column-indexed positions that have the same value of $j \bmod q$ (but different from the value of $i \bmod q$) should be an even number. When r is six, q is four. When r is larger than or equal to seven, q is the smallest power of two larger than or equal to r.
5) The number of 1's in each row should be an integer as close to the ratio of the number of 1's in the H-matrix to the number of rows.
6) One-weight columns should be assigned as check bit columns.
7) Data bit columns should be selected in order to reduce the number of 1's in the H-matrix.

The first and second constraints guarantee that syndrome becomes a non-zero vector when a single bit error occurs and all single bit errors are correctable. The third constraint guarantees that all adjacent double bit errors are correctable. The fourth constraint is the essential constraint for simultaneous testing.

By the fourth constraint, the *r* check bits should have the same values of the *r* lower data bits when a *q*-bit sequence is repeated in DBs. The fifth constraint makes each row have a similar number of 1's, thereby reducing the delay of the check bit generator. The seventh constraint reduces the number of 1's in the H-matrix, leading to a reduction in both the area overhead and the power consumption of the check bit generator.

When *r* is six, *q* cannot be eight because it is impossible to construct the H-matrix. In the (22, 16) proposed DAEC-TAEC code, *q* is not inevitably eight but rather four, demonstrates a manually constructed example of the H-matrix for the (22, 16) proposed SEC-DAEC code and its 6 × 4 characteristic matrix showing the numbers of 1's in column-indexed positions that are such that *j mod* 4 is the same value in each row of the H-matrix excluding the identity matrix, respectively. Moreover, the resultant matrix comprised of XOR-sums of two adjacent H- matrix columns is shown in Fig. 2(c). It is confirmed that the columns in the H-matrix and the XOR-sums of two adjacent columns are independent of each other. The 16 data bit columns are selected in order to satisfy the constraints. In the zeroth row of the H-matrix (*i mod* 4 = 0), the number of 1's in the zeroth, fourth, eighth, and 12th column-indexed positions that are such that *j mod* 4 = 0 is an odd number (three), and the numbers of 1's in the other column-indexed positions such that *j mod* 4 = 1, 2, or 3 are even numbers (two, two, and zero, respectively). In the first, second, third, fourth, and fifth rows, the numbers of 1's in column-indexed positions that are such that *j mod* 4 is the same as *i mod* 4 are also odd numbers.

During normal operations of memory with the (22, 16) proposed DAEC-TAEC code, check bits are generated using the following relations:

$c0 = d1 + d4 + d5 + d8 + d10 + d12 + d14$ $c1 = d0 + d2 + d4 + d6 + d7$

$+ d11 + d13$ $c2 = d1 + d3 + d7 + d9 + d14$

$c3 = d0 + d1 + d2 + d4 + d10 + d13 + d15$

$c4 = d2 + d5 + d6 + d9 + d12$

$c5 = d0 + d3 + d5 + d7 + d8 + d11 + d15$

A 4-bit sequence is repeated in 16-bit DBs during memory test, the relations of data bits are as follows:

$d0 = d4 = d8 = d12$ $d1 = d5 = d9 = d13$ $d2 = d6 = d10 = d14$

The proposed DAEC-TAEC code for more than 32 data bits per ECC word can be simply expanded to accommodate a larger number of data bits in meeting the proposed seven constraints, demonstrate manually constructed examples of the H- matrices of the (39, 32) and (72, 64) proposed DAEC-TAEC codes and their characteristic matrices showing the numbers of 1's in column-indexed positions that are such that *j mod* 8 is the same value in each row of the H-matrix excluding the identity matrix respectively. In the (39, 32) and (72, 64) proposed DAEC-TAEC codes, *q*'s are both eight which is the smallest power of two larger than or equal to *r*.

V. CONCLUSION

A new DAEC-TAEC code is proposed to test the most general memory fault models such as single-cell faults, interword CFs, and intraword CFs in both data bit and check bit arrays simultaneously. The proposed DAEC-TAEC code generates the identical DB patterns for data bit and check bit arrays. The test time and hardware overheads required for separate check bit array tests are reduced by simultaneous testing using the proposed DAEC- TAEC codes reduces. Moreover, the reduction in the number of 1's in the H-matrix of the proposed DAEC-TAEC reduces hardware overhead. As a benefit for using the proposed DAEC-TAEC code in memories, the cost of testing highly reliable memories with single bit error and adjacent double bit error correcting capabilities can be made more practical.

===

REFERENCES

[1] R. Baumann, "Soft errors in advanced computer systems," *IEEE Des. Test Comput.*, vol. 22, no. 3, pp. 258–266, May/Jun. 2005.

[2] R. C. Baumann, "Radiation-induced soft errors in advanced semiconduc-tor technologies," *IEEE Trans. Device Mater. Rel.*, vol. 5, no. 3, pp. 305– 316, Sep. 2005.

[3] P. E. Dodd, M. R. Shaneyfelt, J. R. Schwank, and J. A. Felix, "Current and future challenges in radiation effects on CMOS electronics," *IEEE Trans. Nucl. Sci.*, vol. 57, no. 4, pp. 1747– 1763, Aug. 2010.

[4] M. Franklin and K. K. Saluja, "Pattern sensitive fault testing of RAMs with built-in ECC," in *Proc. Int. Symp. Fault-Tolerant Comput.*, 1991, pp.385–392.

[5] K. Kushida, N. Otsuka, O. Hirabayashi, and Y. Takeyama, "DFT tech-niques for memory macro with built-in ECC," in *Proc. IEEE Int. Workshop Mem. Technol., Des., Testing*, 2005, pp. 109–114.

[6] P. Ramanathan, K. K. Saluja, and M. Franklin, "Zero cost testing of check bits in RAMs with on-chip ECC," in *Proc. IEEE VLSI Test Symp.*, 1992, pp. 292–297.

[7] P. Ramanathan, K. K. Saluja, and M. Franklin, "Testing check bits at no cost in RAMs with on-chip ECC," *IEE Proc. Comput. Digit. Tech.*, pp.304–312, Oct. 1993.

[8] S. Cha and H. Yoon, "Single-error-correction code for simultaneous testing of data bit and check bit arrays for word-oriented memories," *IEEE Trans. Device Mater. Rel.*, vol. 13, no. 1, pp. 266–271, Mar. 2013

==

Ayyappan S.
Assistant Professor
ayps23@gmail.com

Srividhya B., M.E. Student
srivalar92@gmail.com

Department of Electronics & Communication Engineering
Sri Subramanya College of Engineering & Technology
NH - 209, Sukkamanaickenpatti
Palani 624615
Tamil Nadu
India

MULTIPLE ERROR DETECTION AND CORRECTION OF PARALLEL FIR FILTER BASED ON REDUCED PRECISION LOGIC

Jeswin Baby.T., M.E.
Chitra.E.N., M.E. Student

===

Abstract

In this paper, we propose efficient methods for error correction which provides better performance for parallel finite impulse response filters. Reduced-precision redundancy (RPR) has been shown to be a viable alternative to triple modular redundancy (TMR) for digital circuits. This paper builds on previous research by offering a detailed analysis of the implementation of RPR on FPGAs to improve reliability in soft error environments. Example implementations and fault injection experiments demonstrate the cost and benefits of RPR, showing how RPR can be used to improve the failure rate by up to 200 times over an unmitigated system at costs less than half that of TMR. A novel method is also presented for improving the error-masking ability of RPR by up to 5 times at no additional hardware cost under certain conditions. This research shows RPR to be a very flexible soft error mitigation technique and offers insight into its application on FPGAs.

Key words: Reduced Precision redundancy, Triple Modular redundant, FPGA (Field Programmable Gate Array.)

I. INTRODUCTION

A number of techniques can be used to protect a circuit from errors. Those range from modifications in the manufacturing process of the circuits to reduce the number of errors to adding redundancy at the logic or system level to ensure that errors do not affect the system functionality. To add redundancy, a general technique known as triple modular redundancy (TMR) can be used. The TMR, which triplicates the design and adds voting logic to correct errors, is commonly used. However, it more than triples the area and power of the circuit, something that may not be acceptable in some applications. When the circuit to be protected has algorithmic or structural properties, a better option can be to exploit those properties to implement fault tolerance.

Digital filters are one of the most commonly used signal processing circuits and several techniques have been proposed to protect them from errors. Most of them have focused on finite-impulse response(FIR) filters. To operate reliably in space, a hardware mitigation strategy, such as triple modular redundancy (TMR), must be applied. TMR, however, is very expensive and requires three times more hardware resources than an unmitigated circuit. Motivated by the observation that an FPGA-based radio comprises mostly arithmetic operations, this paper explores the application of reduced precision replica (RPR) to the problem. The metric used to evaluate the effectiveness of RPR is the bit error rate (BER) achieved by the FPGA-based radio. To fully evaluate the benefits of RPR on a communications system, the impact of ionizing radiation on BER must be well understood

RPR is a relatively new technique and is more difficult to implement than TMR. There are a number of important design decisions that must be made for each circuit protected by RPR. These choices include selecting the precision of the reduced-precision circuits and determining the threshold for detecting low-magnitude errors. This paper expands on previous work by clarifying the design space of these design choices and defining the trade-offs associated with these parameters. By understanding the impact of these design choices, more efficient SEU mitigation can be achieved. Using this insight, this paper introduces a new method to increase the effectiveness of RPR by up to 5 times for some systems with no additional hardware cost.

A. Single Event Upsets

SRAM-based (static random access memory) FPGAs consist of a large array of memory cells. These memory cells hold both user data and configuration data that define the operation of the circuit. Charged particles affect these cells by occasionally inverting the contents of a particular cell. To protect an FPGA design from SEUs, several fault tolerance techniques are typically used. First, the upsets themselves are periodically repaired to prevent upset accumulation. Hardware redundancy techniques involve the use of additional, redundant hardware to mask the effects of SEUs. TMR uses three copies of the circuit and voting to choose the correct output. Figure 1 shows a simplified block diagram of a digital filter protected with TMR. As long as two of the three modules are operating correctly, the final output is correct. TMR is popular because it is straightforward to implement and provides very effective protection for any type of design.

II. TRIPLE MODULAR REDUNDANCY

Triple Modular Redundancy has three identical logic circuits (logic gates) are used to compute the specified Boolean function. The set of data at the input of the first circuit are identical to the input of the second and third gates. In computing, triple modular redundancy, sometimes called triple-mode redundancy.TMR is a fault-tolerant form of

N-modular redundancy, in which three systems perform a process and that result is processed by a majority-voting system to produce a single output. If any one of the three systems fails, the other two systems can correct and mask the fault.

The TMR concept can be applied to many forms of redundancy, such as software redundancy in the form of N-version programming, and is commonly found in fault-tolerant computer systems. Some ECC memory uses triple modular redundancy hardware (rather than the more common Hamming code), because triple modular redundancy hardware is faster than Hamming error correction software.

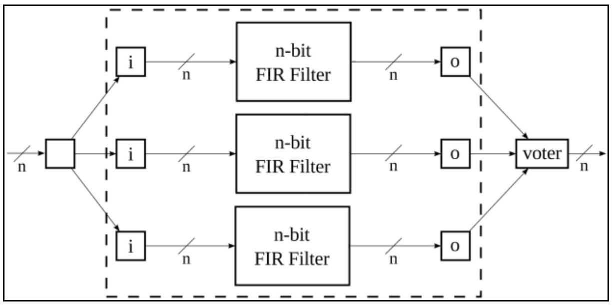

Fig. 1. Simplified block diagram of n-bit FIR filter protected with TMR

A. TMR with Hamming Code

The new technique is based on the use of the ECCs. A simple ECC takes a block of k bits and produces a block of n bits by adding n−k parity check bits. The parity check bits are XOR combinations of the k data bits. By properly designing those combinations it is possible to detect and correct errors. As an example, let us consider a simple Hamming code with

k = 4 and

n = 7. In this case, the three parity check bits p1, p2, p3 are computed as a function of the data bits d1, d2, d3, d4 as follows:

$$p1 = d1 \oplus d2 \oplus d3$$

$$p2 = d1 \oplus d2 \oplus d4$$

$$p3 = d1 \oplus d3 \oplus d4$$

For the case of four filters y1, y2, y3, y4 and the Hamming code, the check filters would be

$$z1[n] = \sum^{\infty}_{l=0} (x1[n-l] + x2[n-l] + x3[n-l]) \cdot h[l]$$

$$z2[n] = \sum^{\infty}_{l=0} (x1[n-l] + x2[n-l] + x4[n-l]) \cdot h[l]$$

$$z3[n] = \sum^{\infty}_{l=0} (x1[n-l] + x3[n-l] + x4[n-l]) \cdot h[l]$$

B. Error Detection and Correction

$$z1\,[n] = y1\,[n] + y2\,[n] + y3[n]$$

$$z2\,[n] = y1\,[n] + y2[n] + y4[n]$$

$$z3\,[n] = y1\,[n] + y3[n] + y4[n].$$

For example, an error on filter y1 will cause errors on the checks of z1, z2, and z3. Similarly, errors on the other filters will cause errors on a different group of zi. Therefore, as with the traditional ECCs, the error can be located and corrected.. For example, when an error on y1 is detected, it can be corrected by making

$$Y\,c1[n] = z1[n] - y2[n] - y3[n].$$

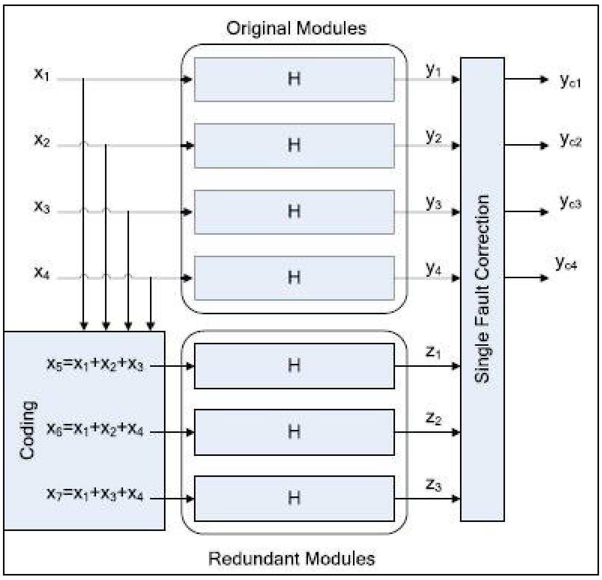

Fig 2: Four Filters and Hamming Codes.

Similar equations can be used to correct errors on the rest of the data outputs and calculate s = yHT to detect errors. For the filters, correction is achieved by reconstructing the erroneous outputs using the rest of the data and check outputs Then, the vector s is also used to identify the filter in error. In our case, a nonzero value in vector s is equivalent to 1 in the traditional Hamming code

Table1: Error Location in the Hamming Code

S1 S2 S3	ERROR BIT POSITION	ACTION
000	NO ERROR	NONE
111	d 1	CORRECT d1
110	d 2	CORRECT d2

101	d 3	CORRECT d3
011	d 4	CORRECT d4
100	P 1	CORRECT p1
010	P 2	CORRECT p2
001	P 3	CORRECT p3

III. THE PROPOSED WORK

A. REDUCED PRECISION REDUNDANCY

RPR is a redundancy technique similar to TMR that requires less hardware overhead by using reduced-precision (RP) arithmetic in two of its three replicas. It takes advantage of the fact that RF arithmetic can be a good estimate of computations that use higher precision. When TMR protects the entire circuit and provides an error-free output, RPR simply limits the error at the output of a module.

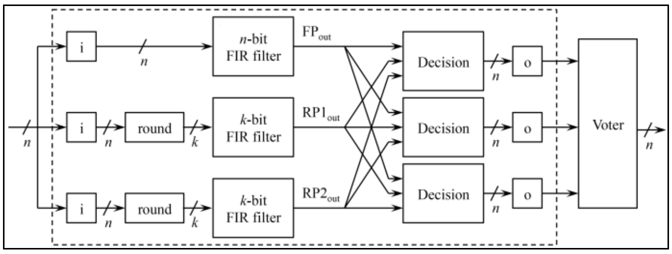

Fig. 3.Block diagram of an n-bit FIR filter protected with RPR using k-bit RF filters (k<n)

. In this paper, a set of four parallel filters with 16 coefficients are used. The input data x[n] and coefficients bi are quantized to 8 bits. The filter output is quantized with 16 bits. Error is introduced at the output of fourth filter y4 [n].Using RPR technique, single bit error is detected and corrected. Verilog Code is written and simulated in ModelSim and Xilinx ISim and implemented in Virtex 5 xc5vlx110t-2ff1136.

RPR is able to reduce the negative impact of SEUs on numerical computations; none of this work has investigated the benefits of RPR on the performance of a communication system. This paper measures the effects of soft errors on the BER of a communications receiver. RPR is applied to two different styles of communication receivers, and the BER of the receivers protected by RPR are compared against a receiver without RPR. In addition to RPR critical clock and reset signals are included in the mitigation approach to maximize the benefits of RPR.

B. Implementation of RPR with TMR

It shows a block diagram of an n-bit finite impulse response (FIR) filter (a filter with n-bit registers and coefficients) protected with RPR. Note that the decision blocks and outputs can be triplicates as well to avoid single points of failure in those modules. The outputs of the three identical decision blocks are voted on, as in the TMR system.

To determine the presence of an error, the decision block compares the outputs of the full-precision (FP) filter (FPout) with the outputs of the two RP filters (RP1out and RP2out) as follows:

if ((FP out -RP1out>Th) AND (RP1out =RP2out)

Output= RP2out

else

Output = FP out.

In other words the FP output is used when no error is found or when the two RP modules disagree. Otherwise, the RP output is used, which provides an estimate of the correct FP output. RPR, in the form presented here, has two main parameters that can be adjusted. The impact of these parameter settings can be understood in terms of the arithmetic error.

€= FP true RP true

Where FP true and RP true are the outputs of the FP and RP filters, respectively, when no SEU is present. First, the size of the RP modules can be modified. The size of the RP filters is measured by the bit-width of the filter input signal, k. A larger RP filter gives a better estimate of the FP filter. This results in a better detection of errors in the FP filter and a lower €. A smaller RP filter is desirable because a smaller RP filter reduces the cost of mitigation. The second parameter for RPR is the threshold value Th. A threshold that is too small will cause the RP output to be chosen even when there are no errors in the FP module. To prevent this, Th ¸ max € is required. On the other hand, if Th is too large, the FP output is used even when there are significant errors in that module. In fact any error that is larger than max € must be due to an upset in the system. Consequently, Th should be no greater than this value.

IV RESULTS AND DISCUSSION

The idea of this paper is to compare the resources used by the RPR, ECC and TMR method. From synthesis report of all the three methods it is observed that area utilization is less in RPR method compared to other methods saving 30% of all resource types (slices, flip-flops and LUTs). Delay in proposed scheme is less compared to TMR and more compared to ECC and power consumption is less in RPR compared to other methods. Here the modules are taken as FIR filter simulation results shows the case when two modules are faulty. If module2 is faulty then the module2 output is recovered. The fault free output is copied to the faulty module. However, if module2 is permanent fault, then module2 is discarded if module3 is also faulty, and then the system will be halted. RPR has an advantage over TMR when it is able to sufficiently limit the magnitude of the SEU induced noise at a lower hardware cost. RPR is not suited to protect any type of circuitry as TMR is the decision hardware required.. Operations that can be approximated with less hardware than the standard module are candidates for RPR. RPR has been used to protect arithmetic operations. In addition the approximation and the decision hardware required to choose the final output must not exceed the cost of TMR, otherwise, any advantage of RPR is lost.

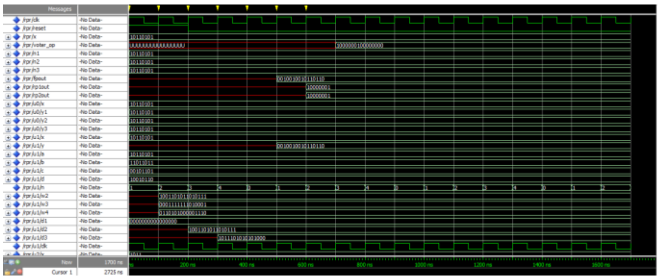

Fig 4: Simulation result of multiple error recovery using RPR

Fig.4 shows the simulation result of multiple error recovery in TMR using RPR technique used in FIR filter All the modes of operation is same as Scan chain multiple error recovery in TMR. The result shows that the proposed technique has greatly reduced in terms of area and power. The main advantage of this technique is that it can detect multiple faults with great minimization in terms of area and delay. The results from these experiments provide concrete evidence that RPR is an effective way of protecting communication circuits from the effects of SEUs.

Table II: Implementation Result

PARAMETER	EXIXTING	PROPOSED
AREA	59.656	37.680
POWER	1364mw	1108mw
DELAY	14.873ns	11.485ns

V CONCLUSION

In this paper, comparison of RPR, TMR and ECC protected Parallel Filters in terms of implementation cost and effectiveness to correct the errors is done. Parallel filters that have same impulse response and with different input and outputs sequences are considered. RPR method is more suitable for multi-bit errors which will also use less area and power compared to other techniques. TMR method can also detect multi-bit errors in any filters but consumes more area and power whereas ECC scheme can detect and correct only single bit error. In Future, utilization of IIR filters instead of FIR filters will be carried out. The extension of the scheme to parallel filters that have the same input and different impulse responses will also be done.

==

REFERENCES

[1] Cummings, M. and Haruyama, S.FPGA in the software radio.*IEEE Communications Magazine*, **37**, 2 (Feb. 1999),108—112.

[2] Caffrey, M. A space-based reconfigurable radio. In T. P. Plaks and P. M. Athanas (Eds.), *Proceedings of the International Conference on Engineering of Reconfigurable Systems and Algorithms* (ERSA ’02), Las Vegas, NV, June 2002, pp. 49—53.

[3] Banu, R. and Vladimirova, T. Fault-tolerant encryption for space applications. *IEEE Transactions on Aerospace and Electronic Systems*, **45**, 1 (Jan. 2009), 266—279

[4] Adell, P., et al Digital control for radiation-hardened switching converters in space. *IEEE Transactions on Aerospace and Electronic Systems*, **46**, 2 (Apr. 2010), 761—770.

[5] Dodd, P. and Massengill, L. Basic mechanisms and modeling of single-event upset in digital microelectronics. *IEEE Transactions on Nuclear Science*, **50**, 3 (June 2003), 583—602

[6] Johnson, E., Wirthlin, M. J., and Caffrey, M. Single-event upset simulation on an FPGA. In T. P. Plaks and P. M. Athanas (Eds.), *Proceedings of the International Conference on Engineering of Reconfigurable Systems and Algorithms* (ERSA), Las Vegas, NV, June 2002, pp. 68—73.

[7] Ostler, P., et al. SRAM FPGA reliability analysis for harsh radiation environments. *IEEE Transactions on Nuclear Science*, **56**, 6 (2009), 3519—3526.

[8] Carmichael, C. Triple module redundancy design techniques for Virtex FPGAs. Xilinx Corporation, Technical Report, Nov. 1, 2001, xAPP197 (v1.0)

[9] Morgan, K., et al. A comparison of TMR with alternative fault-tolerant design techniques for FPGAs. *IEEE Transactions on Nuclear Science*, **54**, 6 (2007),2065—2072.

[10] Huang, K-H. and Abraham, J. Algorithm-based fault tolerance for matrix operations. *IEEE Transactions on Computers*, **C-33**, 6 (June 1984), 518—528.

===

Jeswin Baby. T., M.E.
jeswinbaby@gmail.com

Chitra. E.N., M.E. Student
Kukku.en@gmail.com

Department of Electronics & Communication Engineering
Sri Subramanya College of Engineering & Technology
NH - 209, Sukkamanaickenpatti
Palani 624615
Tamil Nadu
India

==
Engineering & Technology in India www.engineeringandtechnologyinindia.com
Vol. 1:3 April 2016
==

EFFICIENT FACE RECOGNITION METHOD FOR PERSON AUTHENTICATION

Karthick K., M.E.
Sughapriya N., M.E. Student

==

Abstract

In this paper, we propose efficient methods for face recognition which provides better performance for given images which might be taken in presence of different lighting conditions and slight pose variations. Face detection is performed through segmentation and face region coordinate computation. In face recognition process for each training sample the distance metric is learned to find the similarities between images. In order to raise the efficiency of face recognition, a method based on distance metric learning and hybrid neural network (back-propagation (BP) neural network and probabilistic neural network (PNN) integration) was introduced. This method based on FFT in feature extraction, distance metric data is propagated into the HNN and outputs the classification and recognition results by relative voting method. The performance analysis comparison proves the superiority of the proposed method.

Key words: Face detection, face recognition, distance learnng,hybrid neural network.

I. INTRODUCTION

Face recognition can be categorized into two classes: face verification and face identification. The first aims to verify whether a given pair of face images/video is from the same person or not, and the second aims to recognize the given face image from a gallery set and find the most matched one. In this work, we focus on face detection and identification, which aims to determine whether a given pair of face images captured in unconstrained environments is from the same person or not. Images containing faces are essential to intelligent vision-based human computer interaction, person identification and verification.

Research efforts in face processing include face recognition, face tracking, pose estimation, and expression recognition. However, many reported methods assume that the faces in an image or an image sequence have been identified and localized. To build fully automated systems that analyze the information contained in face images, robust and efficient face detection algorithms are required. The purpose of face authentication is to verify the claim of the identity of an individual in an input image, while face tracking methods continuously estimate the location and possibly the orientation of a face in an image sequence in real time [7], [3].Facial expression recognition concerns identifying the affective states (happy, sad, disgusted, etc.) of humans. Evidently, face detection is the first step in any automated system which solves the above problems. We focus on face detection and recognition methods rather than tracking methods.

II. FACE RECOGNITION TECHNOLOGY

Perfecting face recognition technology is dependent on being able to analyze multiple variables, including lighting, image resolution, uncontrolled illumination environments, scale, orientation, pose (out-of-plane rotation).

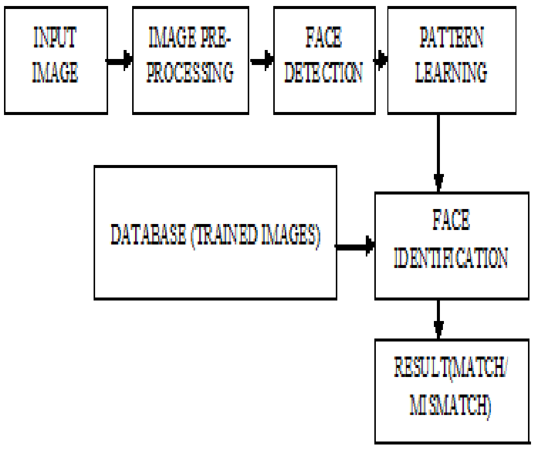

Fig. 1. Block diagram for face recognition process

Face detection should be performed before recognition system. This is done to extract relevant information for face and facial expression analysis. A face is represented as an array of pixel intensity values suitably pre-processed in appearance based approaches (texture). This array is then compared with a face template using a suitable metric [4]. Face identification generates the final output of complete face- recognition system: the identity of the given face image. Based on normalized face image and facial feature locations derived from previous stages, a feature vector is generated from given face and compared with a database of known faces. If a close match is found, the algorithm returns the associated identity.

A. Applications

Person authentication can be performed based on face image recognition technology in the server database or user login. Face-detection programs in digital photo-management software are used to tag photos and organize photo collections. Most digital cameras today have built-in face detectors that improve auto-focusing and auto-exposure. There are also prototypes of applications that use the built-in camera in the mobile phone. After taking a snapshot of the crowd, for example, the application searches all available social networks to identify faces. If matches are located, that profile information can then be displayed almost in real time while you're walking down the street.

B. Challenges associated with face recognition

The images of a face vary due to the pose(relative camera- face pose some facial features such as an eye or the nose may become partially or wholly occluded),presence or absence of structural components, facial expression, occlusion(faces may be partially occluded by other objects),image orientation(face images directly vary for different rotations about the camera’s optical axis),imaging conditions When the image is formed, factors such as lighting and camera characteristics (sensor response, lenses) affect the appearance of a face. There are many closely related problems of face detection. Face localization aims to determine the image position of a single face; this is a simplified detection problem with the assumption that an input image contains only one face . The goal of facial feature detection is to detect the presence and location of features, such as eyes, nose, nostrils, eyebrow, mouth, lips, ears, etc., with the assumption that there is only one face in an image [2].

III. THE PROPOSED WORK

A. Pre-processing steps for an image

The placement of the light sources can make a considerable difference in the type of message that is being presented. Multiple light sources can wash out any wrinkles in a person's face, for instance, and give a more youthful appearance. The goal of illumination correction is to remove uneven illumination of the image caused by sensor defaults non uniform illumination of the scene, or orientation of the object- surface.

Illumination correction is based on background subtraction This type of correction assumes the scene is composed of an homogeneous background and relatively small objects brighter or darker than the background. There are two major types of background subtraction techniques depending on whether the illumination model of the images can be given as additional images or not. In image processing, to smooth a data set is to create an approximating function that attempts to capture important patterns in the data, while leaving out noise or other fine-scale structures/rapid phenomena. The probability maps are obtained, the decision rule is applied to each pixel of the image to classify it either as a skin or non-skin pixel. In order to speed up the process, the original image is subsampled by a factor of 4 before the skin segmentation routine is applied. After skin segmentation, the image mask is up-sampled back to the original image size for further processing.

Fig. 2. Illumination controlled and smoothed images

In smoothing, the data points of a signal are modified so individual points (presumably because of noise) are reduced, and points that are lower than the adjacent points are increased leading to a smoother signal. Smoothing may be used in two important ways that can aid in data analysis by being able to extract more information from the data as long as the assumption of smoothing is reasonable and by being able to provide analyses that are both flexible and robust.

B. Face detection

Face detection takes images as input and locates face areas within these images. This is done by separating face areas from non-face background regions. Facial feature extraction locates important feature positions within a detected face this is achieved by distance metric learning using fast fourier transform(FFT). Feature extraction simplifies face region normalization where detected face aligned to coordinate framework to reduce the large variances introduced by different face scales and poses. The accurate locations of feature points sampling the shape of facial features provide input parameters for the face identification. When a raw or filtered image is considered as input to a pattern classifier (HNN). The classes of face and non-face images are decidedly characterized by multimodal distribution functions and effective decision boundaries are likely to be nonlinear in the image space.

Fig. 3. Proposed face detection process (segmentation, noise eroded, region fill, detected region, face detected images)

Original image and its size are read, skin segmentation is performed, suspected face regions set to 1 and non-face regions set to 0,image is Converted into the BW format, noise eroded, holes are filled to get fully connected face regions, each connected region in the BW image are Labeled ,face regions are filtered out, the coordinates of each face region are computed, each detected face is highlighted by a box around face region.

C. Feature Extraction

Feature transform (FFT) in used to detect and describe local features in images. The key points of objects are first extracted from a set of reference images and stored in a database. An object is recognized in a new image by individually comparing each feature from the new image to this database and finding candidate matching features based on distance[1], of their feature vectors. From the full set of matches, subsets of key points that agree on the object and its location, scale, and orientation in the new image are identified to filter out good matches. In Dense SIFT , SIFT descriptors are densely sampled on each 16 × 16 patch without overlapping and. In LBP, each image divided into 8×15 non- overlapping blocks, where the size of each block is 10×10,SparseSIFT includes localization of nine fixed landmarks in each image and extracted SIFT features over three scales at these landmarks by following . Then, we concatenate these SIFT descriptors to form one feature vector. For these three features, FFT is performed to project each feature into a feature subspace.

D. Hybrid Neural Network

The first stage consists of two parallel sub networks in which the inputs are intensity values from an original image and intensity values from filtered image. The inputs to the second stage network consist of the outputs from the sub networks and extracted feature values such as the standard deviation of the pixel values in the input pattern, a ratio of the number of white pixels to the total number of binarized pixels in a window, and geometric moments.

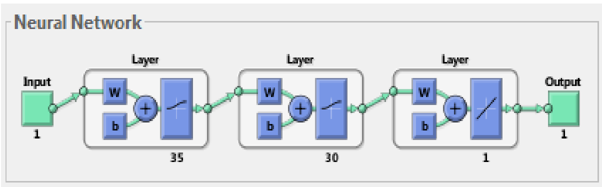

Fig. 4. Layer diagram of proposed neural network

An output value at the second stage indicates the presence of a face in the input region. Neural network is used to find a discriminate function to classify face and non-face patterns using distance measures. There are two major components: multiple neural networks (to detect face patterns) and a decision making module (to render the final decision from multiple detection results). Given a test pattern, the output of the trained neural network indicates the evidence for a non- face(close to 0) or face pattern (close to 1). To detect faces anywhere in an image, the neural network is applied at all image locations.

In HNN When an input is present, the first layer computes the distance from the input vector to the training input vectors.This produces a vector where its elements indicate how close the input is to the training input. The second layer sums the contribution for each class of inputs and produces its net output as a vector of probabilities. Finally, a compete transfer function on the output of the second layer picks the maximum of these probabilities, and produces a 1 (positive) for that class and a 0 (negative identification) for non-targeted classes. Training set contains face images collected from various face databases. Each image is divided into small sub images and then each one is tested separately using a HNN. The network is trained with multilayer back propagation neural networks (BPNN). FFT feature values of faces that represent the data set of face candidates obtained ,are fed into PNN to classify whether original image included in the DB. The PNN input is feature vector based on FFT.

IV RESULTS AND DISCUSSION

The proposed method for human face recognition is implemented by using MATLAB software in programming level. MATLAB is a data analysis and visualization tool which has been designed with powerful support for matrices and matrix operations. As well as this, MATLAB has excellent graphics capabilities, and its own powerful programming language. The test/input image is preprocessed face region is detected, image pattern generated and then compared with the database (consists of trained images whose pattern are formed) of images to identify whether the input image belong to the database images. Finally image match or mismatch status is declared through a message/dialogue box in the text or voice format.

The detected face is highlighted by a box around face region. Face identification generates the final output of complete face-recognition system: the identity of the given face image. Based on normalized face image and facial feature locations derived from previous stages, a feature vector is generated from given face and compared with a database of known faces. If a close match is found, the algorithm returns the associated identity.

The HNN is used to represent function using arbitrary decision surfaces by utilizing nonlinear activation functions. Their experiments showed that the methods show closer performances for the classification in face and non-face space, and the method has achieved high detection rates and an acceptable number of false negatives and false positives face detection. The advantage of using neural networks for face detection is the feasibility of training a system to capture the complex class conditional density of face patterns. The usage of HNN increases accuracy compared to the other type of neural networks. The HNN classification implementation improves accuracy and almost 87% accuracy is obtained in the face recognition process. This proposed method can be used for both face identification and face verification, incase of face verification the preloaded image and query images are concerned, but for face identification database images and query image are of concern.

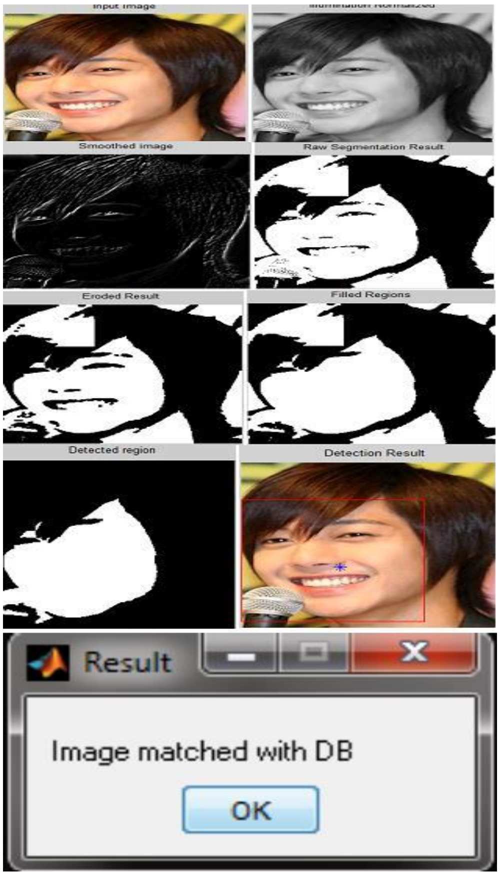

Fig. 5. Proposed Face detection & identification stages

V. CONCLUSION

We proposed the methods for face recognition which could perform efficiently for images that are captured with different lighting conditions, pose variations(provided 75% of visible face view), with the presence or absence of structural components, occlusion. The face detection and face recognition process is performed on the test/input image with the help of proposed methods(distance metric learning, HNN) to improve the accuracy of the face recognition process so that it can be used in security based applications such as person authentication in the organizations, user login through face authentication. This method effectively solves the interferences of illumination, facial pose variation, and as a result improves the classification of the human face recognition ability. The performance analysis result shows the efficacy(87% accuracy) of the proposed methods compared to the other methods.

==

REFERENCES

[1] Jiwen Lu, Gang Wang, Weihong Deng, Kui Jia "Reconstruction-Based Metric Learning for Unconstrained Face Verification", IEEE transactions on information forensics and security, VOL. 10, NO. 1, JANUARY 2015.

[2] O. Barkan, J. Weill, L. Wolf, and H. Aronowitz, "Fast .high dimensionalvector multiplication face recognition," in *Proc. IEEE ICCV*, Dec. 2013,pp. 1960–1967.

[3] M. Belkin and P. Niyogi, "Laplacian eigenmaps and spectral techniques for embedding and clustering," in *Proc. NIPS*, 2001, pp. 585–591.

[4] L. Best-Rowden, H. Han, C. Otto, B. Klare, and A. K. Jain, "Unconstrained face recognition: Identifying a person of interest from a Media collection," *IEEE Trans. Inf. Forensics Security*, to be published.

[5] S. Bickel and T. Scheffer, "Multi-view clustering," in *Proc. ICDM*, 2004, pp. 19–26.

[6] Q. Cao, Y. Ying, and P. Li, "Similarity metric learning for face recognition," in *Proc. IEEE ICCV*, Dec. 2013, pp. 2408–2415.

[7] D. Chen, X. Cao, L. Wang, F. Wen, and J. Sun, "Bayesian face revisited:A joint formulation," in *Proc. ECCV*, 2012, pp. 566–579.

[8] D. Chen, X. Cao, F. Wen, and J. Sun, "Blessing of dimensionality: Highdimensional feature and its efficient compression for face verification," in *Proc. IEEE CVPR*, Jun. 2013, pp. 3025–3032.

[9] Z. Cui, W. Li, D. Xu, S. Shan, and X. Chen, "Fusing robust face region descriptors via multiple metric learning for face recognition in the wild,"in *Proc. IEEE CVPR*, Jun. 2013, pp. 3554–3561.

[10] J. V. Davis, B. Kulis, P. Jain, S. Sra, and I. S. Dhillon,"Information Theoretic metric learning," in *Proc. 24th ICML*, 2007, pp. 209–216.

[11] T. Ahonen, A. Hadid, and M. Pietikainen, "Face description with local binary patterns: Application to face recognition," *IEEE Trans. Pattern Anal. Mach. Intell.*, vol. 28, no. 12, pp. 2037–2041, Dec. 2006.

==

Karthick K., M.E.
Assistant Professor
karthickks.karthick@gmail.com

Sughapriya N, M.E. Student
Sugha07@gmail.com
Electronics & Communication

Department of Electronics & Communication Engineering
Sri Subramanya College of Engineering & Technology
NH - 209, Sukkamanaickenpatti
Palani 624615
Tamil Nadu
India

==
Engineering & Technology in India www.engineeringandtechnologyinindia.com
Vol. 1:3 April 2016
==

MAMMOGRAPHIC MICROCALCIFICATION SEGMENTATION USING FUZZY C MEANS CLUSTERING

Mekala.S., M.E.
Nishanthi.C., M.E. Student
==

Abstract

Breast cancer is one of the major causes of death among women. Mammography is the main test used for screening and early diagnosis. Early detection performed on X-ray mammography is the key to improve breast cancer prognosis. This paper presents a research on mammography images using Morphological operators and Fuzzy c – means clustering for cancer tumor mass segmentation. The first step of the cancer signs detection should be a segmentation procedure able to distinguish masses and micro calcifications from background tissue using Morphological operators and finally fuzzy c- means clustering (FCM) algorithm has been implemented for intensity – based segmentation. This method does not require any manual processing technique for classification, thus it can be assimilated for identifying benign and malignant areas in intelligent way. Moreover it gives good classification responses for compressed mammogram image. The goal of the proposed method is twofold: one is to preserve the details in Region of Interest (ROI) at low bit rate without affecting the diagnostic related information and second is to classify and segment the micro-calcification area in reconstructed mammogram image with high accuracy. The experimental result shows that the proposed model performance is good at achieving high sensitivity of 97.27%, specificity of 94.38% .

Key words: Mammography, Micro calcification, Segmentation, Fuzzy c- means clustering.

I. INTRODUCTION

Breast cancer is the most common malignancy that affects women worldwide and is the leading cause among non-preventable cancer death. The American Cancer Society (ACS) estimates that on an average, in every 15 minutes five women are diagnosed with breast cancer. It is also estimated that one in eight women will be diagnosed with this disease in her lifetime, and 1 in 30 will die from it. Breast cancer is the second most prevalent cancer among Indian women, the first being cervical cancer. In the age group of 30-70 years, one in fifty eight women are affected by this disease and the occurrence is mainly seen in the urban areas. Mammography is the best technique for reliable detection of early, non- palpable, potentially curable breast cancer. As a result of the increasing utilization of mammographic screening, the mortality rate due to this disease was observed to decrease for the first time in 1995. Since the interpretation of mammograms is a repetitive task that requires much attention to minute details, the opinion of radiologists may vary. To overcome this difficulty, during the past decade, the use of image processing technique for Computer Aided Diagnosis (CAD) in digital mammograms has been initiated. This has increased diagnostic accuracy as well as the reproducibility of mammographic interpretation.

II. MICROCALCIFICATION IDENTIFICATION

To investigate the potential correlation between the topology of micro-calcification clusters and their pathological type a series of micro- calcification graphs are constructed to describe the topological structure of micro-calcification clusters at different scales. A set of graph theoretical features are extracted from these graphs for modeling and classifying micro-calcification clusters.

The identification methodology consists of four main phases: estimating the connectivity between micro-calcifications within a cluster using morphological dilation at multiple scales; generating a micro-calcification graph at each scale based on the spatial connectivity relationship between micro- calcifications; extracting multi-scale topological features from these micro-calcification graphs; and using the extracted features to build classifier models of malignant and benign micro-calcification clusters. All image analysis development work was done within MATLAB 2014a.

Morphological dilation is performed on each individual micro-calcification using a disk- shaped structuring element at multiple scales. Here the scale corresponds to the radius of the structuring element measured in pixels. The effect of multi-scale morphological dilation on a micro-calcification cluster is shown. It can be seen that the multi-scale morphological dilation continuously absorbs neighboring pixels into individual micro- calcifications resulting in a change in the connectivity between micro-calcifications within the cluster.

A. MICROCALCIFICATION GRAPH GENERATION

The topology of micro-calcification clusters is represented in graph form. A micro-calcification graph is generated based on the spatial connectivity relationship between micro-calcifications within a cluster. In a micro-calcification graph, each node represents an individual micro-calcification, and an edge between two nodes is created if the two corresponding micro-calcifications are connected or overlap in the 2-D image plane. The node locations in the graphs are in accordance with the original spatial distribution of micro-calcifications within the two clusters, and the node sequences are consistent with those in Fig.3.1, which are sorted in a left-to- right and bottom-to-top direction.

B. MULTI SCALE FEATURE EXTRACTION

After generating micro-calcification graphs over a range of scales, a set of graph theoretical features can be extracted to capture the topological properties of micro-calcification clusters. These features will constitute the feature space for the classification of malignant and benign clusters. Before extracting the topological features of micro- calcification clusters, the following definitions for general graphs are provided. Micro-calcification cluster is more connected. A set of values of the maximum vertex degree against scale which also have an increasing trend from small to large scales are tend toward stability when reaching the maximum value. Similarly, as indicated by the average vertex degree, the maximum vertex degree values for the malignant cluster are also larger than those of the benign cluster. The resulting values of the average vertex eccentricity against scale are plotted. At the first few scales, most micro- calcifications are isolated from others in the cluster, which results in small average eccentricity values (the eccentricity of isolated vertices is set to 0).

C. HIERARCHICAL CLUSTER ANALYSIS

The stepwise procedure attempts to identify relatively homogeneous groups of cases based on selected characteristics using an algorithm either algomerative or divisive, resulting to a construction of a hierarchy or treelike structure depicting the formation of clusters. This is one of the most straightforward method.HCA are preferred when the sample size is moderate (under 300 – 400, not exceeding 1000).

D. CLASSIFICATION

The main difficulty here is the accurate extraction of a band of pixels around the segmented mass. Claridge and Richte used the Polar co- ordinate transform (PCT) to map lesions into polar co-ordinates. A spiculation measure was then computed from the PCT images to discriminate between circumscribed and spiculated masses. Hadjiski classified masses as benign or malignant using texture features computed from the RBST image. They tested the performance of a hybrid classifier consisting of an adaptive resonance theory network cascaded with LDA. They used a set of manually segmented ROIs and reported a higher accuracy with the hybrid classifier than with a back propagation neural network or LDA. Pohlman used six morphological features to classify masses as benign or malignant. To segment the lesions, they used an adaptive region growing technique, which required the selection of manual seed points.

III. PROPOSED WORK

The relative fibroglandular tissue content in the breast, commonly referred to as breast density, has been shown to be the most significant risk factor for breast cancer after age. This work presents a novel multi-class fuzzy c-means (FCM) algorithm for fully-automated identification and quantification of breast density, optimized for the imaging characteristics of digital mammography. The proposed algorithm involves adaptive FCM clustering based on an optimal number of clusters derived by the tissue properties of the specific mammogram, followed by generation of a final segmentation through cluster agglomeration using linear discriminant analysis. When evaluated on 80 bilateral screening digital mammograms, a strong correlation was observed between algorithm- estimated PD% and radiological ground-truth of r=0.83 (p<0.001) and an average Jaccard spatial similarity coefficient of 0.62. These results show promise for the clinical application of the algorithm in quantifying breast density in a repeatable manner. Besides of analysing performance of AIS, we also compared the performance of AIS as a data reduction method on two real world classification problems. They are Diabetes Disease and Breast Cancer classification problems. The related datasets were taken from the UCI data mining repository. In these experimentations however, train & test data partitioning was conducted in a different way. Firstly, the training and testing data were determined and then the training data were reduced with AIS and FCM methods. In this step, data were reduced so that approximate compression ratios of 10%, 20%, 30%, 40%, 50%, 60%, 70%, 80%, 90%, 95%and 98% were obtained.

A. METHODOLOGY

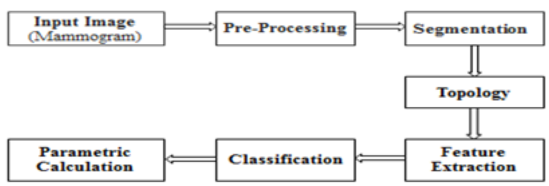

Fig.1Basic Flow Diagram

B. PREPROCESSING

The preprocessing phase of the proposed system is focused at removal of channel noise, enhancing the contrast and for removal of the background of mammogram images. The ROI containing abnormalities are separated from the background and further features are computed from the ROI. Channel noise is considered as salt and pepper noise which is removed using median filter (Jae, 1990) whereas histogram equalization technique (Nunes*et al.*, 1999) is used to enhance the contrast and Otsu Global threshold (Otsu, 1979) is used for extracting the background from ROI

C. SEGMENTATION

This section details the segmentation of mammograms for identifying the cancer in breasts. The proposed approach utilizes mathematical morphology operations for the segmentation. The morphological operations are applied on the grayscale mammography images to segment the abnormal regions. Erosion and dilation are the two elementary operations in

Mathematical Morphology. An aggregation of these two represents the rest of the operations . The symbols _, Θ, o, and • , respectively denote the four fundamental binary morphological operations: dilation, erosion, opening, and closing. A function $f(x, y)$ denotes the image, where (x, y) _ $R2$ or Z2 ,or simply f , and the function $h(x, y)$, or h will act as the structuring element.

D. FUZZY C-MEANS ALGORITHM

Fuzzy C-means algorithm is also called as ISODATA. It was most frequently used in pattern recognition. Fuzzy C-mean is the method using in clustering. It is using one piece of data to belong to two or more clusters. It always based on minimization of objective functions to achieve a good classification.

E. SEGMENTATION ALGORITHM USING FUZZY-C MEANS ALGORITHM

Step 1: Read the input mammogram image and decide the number of clusters C.

In this C=3

Step 2: Assign the value of ε(threshold) and number of iteration as T.

Step 3: Assign the cluster centres,

$V^{(i)}=[V^{(i)},V_2^{(i)}....V_c^{(i)}]$

Step 4: Evaluate the degree of membership function

Step 5: Evaluate the centres of clusters $V^{(q+1)}$

Step 6: If $\|V^{(q+1)} - VV^{(q)}\| <$ i or the number of iteration q>1 then write the Output as clustering output, or else q=q+1 go to step4

Step 7: Extract the cancerous area from clustered output; perform morphological operations to calculate the area of the cancerous region.

F. PERFORMANCE EVALUATION OF FUZZY C-MEANS

The most important difference is that in FCM, each has a weighted associated with a specify cluster so, a point doesn't have cluster as much as a little or more association to cluster. It was very determine by increase distance to the center of the cluster. FCM will tend to run slower than K-means, since it is actually doing more work. Every point is calculated with each cluster, and many operations are involved in each evaluation.

In this proposed work we make these differences or weakness our strong point for full detection of breast cancer from this we were able to find the messes and the cancer area.

G. FEATURE EXTRACTION

As the case for masses, the features used for the diagnosis of calcification can be viewed as either capturing morphological or texture information. Researchers have reported that morphology is one of the most important clinical factors in calcifications diagnosis. Features for calcification classification can also be organized in terms of whether the describe properties of the cluster as a whole or of the individual calcifications that make up the cluster.

IV. RESULT

The proposed method is implemented by using MATLAB software in programming level. MATLAB is a data analysis and visualization tool which has been designed with powerful support for matrices and matrix operations. As well as this, MATLAB has excellent graphics capabilities, and its own powerful programming language. When dealing with mammograms, it is known that pixels of tumor regions tend to have maximum allowable digital value. Based on this information, morphological operators are used such as Dilation is used to detect the possible clusters which contain masses. Image features are then extracted to remove those clusters that belong to background or normal tissue as a first cut..The fuzzy c-means clustering algorithm is used as a segmentation strategy to function as better classifier & aims to class data into separate groups according to their characteristics.

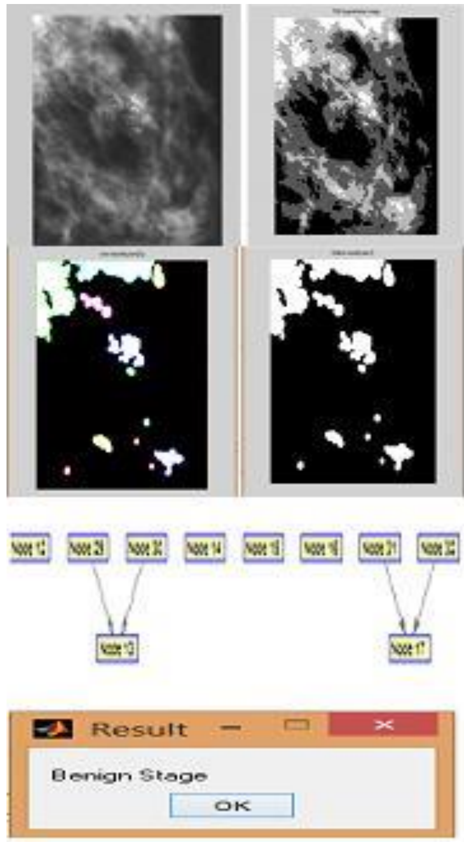

Fig 2. Processing and indication stages

V. CONCLUSION

The early diagnosis through regular screening and timely treatment has been shown to prevent cancer. In this paper we have presented a novel approach to identify the presence of breast cancer mass in mammograms. The proposed work utilizes fuzzy c- means clustering for clear identification of clusters. The FCM is a new approach, using this we have successfully detected the breast cancer masses in mammograms. This result indicates that this system can facilitate the doctor to detect breast cancer in the early stage of diagnosis process.

==

REFERENCES

[1] American Cancer Society, Global Cancer Facts & Figures, 2nd ed. Atlanta, GA, USA: Amer. Cancer Soc., 2011, pp. 11–12.

[2] Eurostat, Health Statistics Atlas on Mortality in the European Union. Office for Official

Publications of the European Union, 2009, pp. 91–93.

[3] American Cancer Society, Breast Cancer Facts & Figures 2011– 2012. Atlanta, GA, SA: Amer. Cancer Soc., 2011, pp. 11–15.

[4] National Comprehensive Cancer Network, NCCN Clinical Practice Guidelines in Oncology: Breast Cancer Screening and DiagnosisNCCN Clinical Practice Guidelines in Oncology: Breast Cancer Screening and Diagnosis, 2012.

[5] Cancer Research U.K. (2012, Aug.) "Who is screened for breast cancer?"

[6] L. Shenet al., "Application of shape analysis to mammographic calcifications," IEEE Trans. Med. Imag., vol. 13, no. 2, pp. 263–274, Jun. 1994.

[7] P. Dhawanet al., "Analysis of mammographic micro calcifications using gray-level image structure features," IEEE Trans. Med. Imag., vol. 15, no. 3, pp. 246–259, Jun. 1996.

[8] H. D. Cheng et al., "Computer-aided detection and classification of micro calcifications in mammograms: A survey," Pattern Recog., vol. 36, no. 12, pp. 2967–2991, 2003.

[9] Y. Ma, et al., "A novel shape feature to classify micro calcifications," in Proc. 17th IEEE Int. Conf. Image Process., 2010, pp. 2265–2268.

==

Mekala. S., M.E.
mekala.4138@gmail.com

Nishanthi. C., M.E. Student
nishachinnasamy93@gmail.com

Department of Electronics & Communication Engineering
Sri Subramanya College of Engineering & Technology
NH - 209, Sukkamanaickenpatti
Palani 624615
Tamil Nadu
India

==
Engineering & Technology in India www.engineeringandtechnologyinindia.com
Vol. 1:3 April 2016
==

Unsupervised Change Detection of Urban Land Use and Land Cover Change in SAR Images

R. Padmapriya, M.E.
Dr. V. Ilankumaran

==

Abtsract

Remote sensing plays an important role in analysis of natural resources on the earth and to monitor the land use and land cover changes .Now a days this LULC mapping is of great significance in scientific planning and management because the land space destruction is essential where change detection aims at identifying the change that have ocuured in an area at two different times. This paper proposes a unsupervised monitoring based on undecimated discrete wavelet transform . Initally from the co-registered images wavelet features are extracted using UDWT.change vector analysis is applied next on the two temporal images. As a result change detection map is created.

Keywords: Change Detection; LULC; UDWT; CVA.

I. INTRODUCTION

In urban areas, regional land use activities much reflect the interaction between man and environment because of mankind's basic economic accomplishments. Distantly sensed satellite images provide a synoptic overview of the whole area in a very short time span. This leads to nippy and truthful illustration of the real world in the finest probable manner. And also, it affords an insight to direct affiliation among shipping, housing, engineering and recreational land uses, besides providing broad-scale records of natural resources and monitoring environmental issues, including land reclamation, restoration, disaster relief, water quality and planning economic development. Change detection is very essential process for monitoring land use and land cover changes which is helpful for managing natural resources. The changes in land use and land cover are normally due to natural and human activities. Several applications are evolved based on remote sensing namely land cover monitoring, land cover change detection, classification, impact assessment and infrastructure planning. For understanding the interactions and relationships between natural phenomena and human, the periodic monitoring of change detection of earth surface is extremely important. In this paper, a novel UDWT transform domain approach to construct change detection binary map is performed initially on two co- registered images. Change Vector Analysis (CVA) is applied next on the two temporal images. As a result, change detection map is produced.

II. RELATED WORKS

Uma Shankar. B. et al. (2011) [1] constructed a wavelet feature based fuzzy classify for land cover detection in multispectral images. Turgay Celik et al. [6] performed unsupervised change detection method using active contour on multiresolution analysis of the difference image. Teerasit Kasetkasem et al. [3] suggested that the observed multi-temporal images can be modeled as Markovian Random Fields (MRFs) to generate a change image by using the maximum posteriori probability decision criterion and the simulated annealing energy minimization method. But this method is not suitable for real-time change detection applications. In order to overcome the high computational complexity, Turgey Celik [5] applied Principal Component Analysis (PCA) and adapted k-means clustering for change detection. This method produced promising results with low computational cost. But, PCA can only separate pair wise linear dependence between data points.

Chan *et al.* [2] proposed the multiresolution analysis of the difference image, together with the level set implementation of the scalar Mumford-Shah segmentation, is employed in Bazi *et al.* [7] to perform the unsupervised change detection. The multiresolution representation of the difference image is achieved by iteratively down sampling the difference image by a factor of two in both directions [7].

In [4] Celik, Dual Tree- Complex Wavelet Transform (DT-CWT) is used to individually decompose each input image into one low-pass subband and six directional high-pass sub bands at each scale of the decomposition.

III. METHODOLOGY

To monitor the changes in terms of land use-land cover using multitemporal images, the methodology followed in this work includes two tasks such as i) Feature Extraction ii) Change map generation using change detection. In the change detection method, extract the differences between the images at different times. Change/ no change map are generated by using direct change detection. The proposed phase architecture shows in below Fig. 1.

- **Image Registration**

It is the process of properly aligning two images into a general co-ordinate system, in order to detect changes between the two images. Initially Scale Invariant Feature Transform (SIFT) is applied to extract key points from images. Images are segmented to regions based on Fuzzy C-means clustering approach which produces clusters. Key points are matched based on their gradient orientations from the clusters of both reference image and target image and finally image warping is performed by applying piecewise linear transformation function.

A. Feature Extraction

Since remotely sensed images are too large to be processed and are redundant in spatial details, the input image is transformed into a reduced representation in terms of features. Here to extract the features UDWT is used. Using Wavelet Transform (WT), the image is decomposed into four subbands. The bands are LL, LH, HL and HH. The LL band is low frequency band; it is represented as an approximation image. The other three bands are represented as high frequency bands in the direction of Vertical (LH), Horizontal (HL) and Diagonal (HH). These bands are represented as detailed images. The UDWT based decomposition involves no downsampling and it is shift invariant. During each level of decomposition four subimages are obtained from each band. These subimages are equal to original image size and are used to reconstruct the images providing frequency and spatial information of the original image. Let X be the original image. Now the multi-resolution representation of the image X is obtained by applying the forward and backward UDWTs with further processing on the wavelet subbands to create XMR = {X0,X1,…..,Xs,….XS}, where the subscript s denotes the resolution index and S is the number of the resolution levels targeted to achieve. The resolution index s=0 corresponds to the original image X itself, i.e., X0=X. The images with a lower resolution index values are more affected by noise; however they are inherited with a large amount of details of the image content. On the other hand, the images with a higher value of resolution index s contain much less/low noise interference and less image content details.

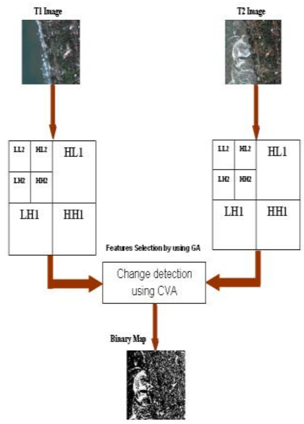

Fig 1.Proposed phase architecture of the work

During the S-level UDWT decomposition of image X, at each level it creates four subbands. To denote the subbands of each kth level, along with resolution index an additional subband index is also used here as ll,lh,hl and hh. So for the kth level decomposition the obtained subbands are labeled as Xk, ll , Xk, lh , Xk, hl and Xk, hh, where k = 1,2,…..S. The baseband Xk, ll is generated by performing low-pass filtering (l) along the rows and columns.

The remaining subbands $X_{k,lh}$, $X_{k,hl}$ and $X_{k,hh}$ are the decomposed high-frequency subbands that are produced by performing low-pass(*l*) (or high-pass (*h*)) filtering along the rows and then high-pass (*h*) (or low-pass(*l*)) filtering along the columns.

The subband $X_{k,ll}$ is further decomposed to produce $X_{k+1,ll}$, $X_{k+1,lh}$, $X_{k+1,hl}$, and $X_{k+1,hh}$. This process will be recursively repeated to the current baseband until the targeted final level (i.e., $k = S$) is reached.

To obtain the $(k+1)_{th}$ level of subband decomposition, only the baseband generated at level *k* is decomposed into subbands. For illustration purpose, the following Fig. 2 shows how the subband $X_{k,\,ll}$ is further decomposed to produce $X_{k+1,\,ll}$, $X_{k+1,\,lh}$, $X_{k+1,\,hl}$ and $X_{k+1,\,hh}$.

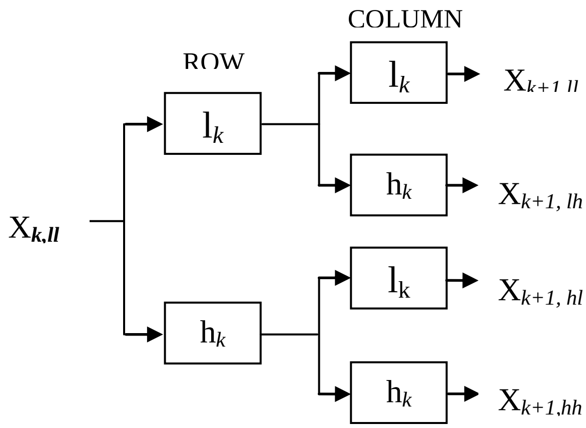

Fig 2.Decomposition process at Level k+1

From the above stage, Table 1 shows the possible combination of both Wavelet Statistical Texture (WST) and Wavelet Co-Occurrence Texture (WCT) features identified for the change detection task.

Table 1: WST AND WCT FEATURES

Wavelet Statistical Texture (WST) FEATURES
Mean, Standard Deviation, Energy
Wavelet Co-Occurrence Texture (WCT) FEATURES
Entropy, Energy, Contrast, Sum Average, Variance, Correlation, Maximum Probability, Inverse Difference Moment, Cluster tendency

Wavelet co-occurrence texture features concentrates on LL, LH, HL bands based on the coefficient values.

B. Feature Selection using GA

Genetic Algorithm (GA) is considered for creating the best solution and it has a set of properties like chromosomes. The purpose of GA is to find the appropriate subset.

1) Fitness Computation

During fitness computation,

- Suppose there are N number of features present in a particular chromosome (i.e., there are total N number of 1's in that chromosome).
- Construct a classifier with only these N features. Here, initially the training data is divided into 3 parts. The above classifier is trained using 2/3 of the training set with the features encoded in that chromosome and tested with the remaining 1/3 part.
- Classifier for the 1/3 training data is calculated.
- Steps 2 and 3 are repeated 3 times to perform 3-fold cross validation.
- The average F-measure value of this 3-fold cross validation is used as the fitness value of the particular chromosome. The objective is to maximize this fitness value using the search capability of GA.

2) Selection

Roulette wheel selection is used to implement the proportional selection strategy.

3) Crossover

Here, we use the normal single point crossover. As an example, let the two chromosomes be:

P1: 0 1 1 0 0 0 1 1 1 0 1 0

P2: 1 0 1 1 0 0 0 0 0 0 1 0

First, a crossover point has to be selected randomly between 1 to 12 (length of the chromosome) by generating some random number between 1 and 12. Let the crossover point, here, be 4. Then after crossover, the two new offsprings are:

O1: 0 1 1 0 0 0 0 0 0 0 1 0 (taking the first 4 positions from P1 and rest from P2)

O2: 1 0 1 1 0 0 1 1 1 0 1 0 (taking the first 4 positions from P2 and rest from P1)

Crossover probability is selected adaptively as 0.5.

4) Mutation

In mutation process, mutation operator is applied to each generation. If the mutated chromosome is superior to both parents it is replaced with similar parent and it is in between the two parents then it replaces the inferior parent otherwise the most inferior chromosome in the population is replaced. Mutation operates by randomly changing one or more components of a selected individual.

Thus the optimally selected features are obtained. In feature selection the bit position '1' indicates that feature is selected and '0' indicates that feature is not selected. These features are used for the input of direct change detection and classification.

C. Change Vector Analysis

Change vector analysis (CVA) method is used to produce the change detection in terms of magnitude and direction of the images. It uses two spectral channels to map both the magnitude of change and the direction of change between the two (spectral) input vectors. The feature vectors for each time period image has to be analyzed. The first step of the CVA method was to generate a feature vector for the images by UDWT. The position variation of the same pixel during different data takes within the space formed by the two axes i.e., determines the magnitude and direction of the spectral change vectors. The next step in the band transformation process into new coordinate axes was to calculate the magnitude of variation among spectral change vectors between the feature vector pairs. The magnitude of vectors was calculated from the Euclidean Distance between the differences in positions of the same pixel from different data takes within the space generated by the axes as follows,

$$R = \sqrt{(yb - ya)^2 \quad (xb - xa)^2} \qquad (1)$$

where R: Euclidean distance,

ya: band values of greenness from T2 image,

yb: band values of greenness from T1 image,

xb: band values of brightness from T2 image and xa: band values of brightness from T1 image.

The phase angle of the vectors, which indicates the type of change that occurred, varies according to the number of components is used. In other words, each vector is a function of the combination of positive or negative changes through channels or spectral bands, which allows to distinguishing 2^n types of changes.

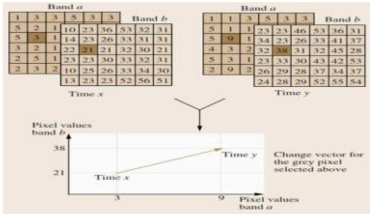

Fig 3. Change Vector Analysis

The changes takes place in two bands a and b is shown in above Fig.3. The main advantage of change vector analysis is ability to process any number of spectral bands desired and to produce detailed change detection information. For example landscape variables, land-cover changes, disaster assessment and conifer forest change.

IV. EXPERIMENTAL RESULTS

For evaluating the proposed work, in Fig. 4, the input images of two different time periods taken in the place of srilanka are considered. These images are of type land cover image.

Fig 4. Input images of two different time periods

The UDWT feature extraction of temporal images contains the Approximation and the detailed images. The following Fig. 5 (a),(b),(c) and (d) shows the one level decomposition of two temporal images. The LL band is an approximation image and LH, HL, HH bands are detailed images. In detail images some of the information is lost.

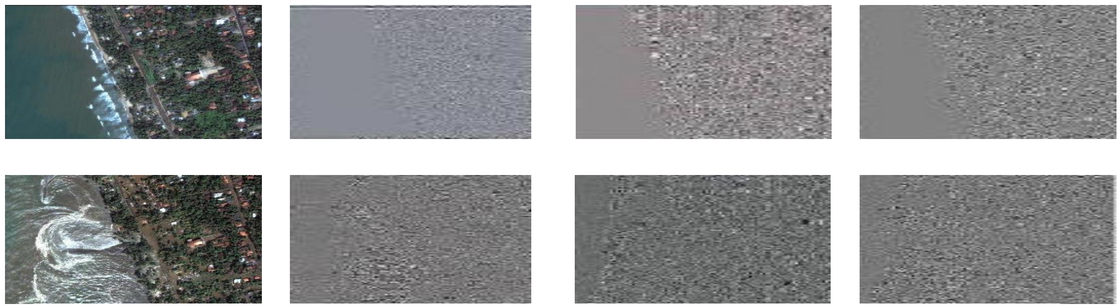

Figure 5 UDWT bands of T1, T2 temporal images (a) LL band (b) HL band (c) LH band (d) HH band

The position variation of the same pixel during different data-takes within the space formed by the axes brightness and greenness which Fig. 6 determines the magnitude and direction of the spectral change vectors.

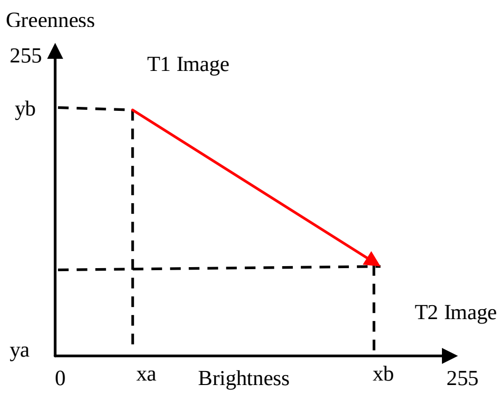

Fig 6.Change Vector obtained from the position variation of the same pixel in different data-taken

A change vector can be described by an angle of change (vector direction) and a magnitude of change from date 1 to date 2 . If a pixel's gray-level values in two images on dates T1, T2 are given by G= $(g1, g2, \ldots, gn)^T$ and H= $(h1, h2, \ldots, hn)^T$, respectively, and n is the number of bands, a change vector is defined as

$$\Delta G = H - G = \begin{pmatrix} h_1 - & g_1 \\ h_2 - & g_2 \\ \cdots & \\ h_n - & g_n \end{pmatrix} \quad (2)$$

where ΔG includes all the change information between the two dates for a given pixel, and the change magnitude is computed with

$$\|\Delta G\| = \sqrt{(h_1 - \ g_1)^2 + (h_2 - \ g_2)^2 + \cdots + (h_n - \ g_n)^2} \quad (3)$$

It represents the total gray-level difference between two dates. The greater $\|\Delta G\|$ is, the higher is the possibility of change. A decision on change is made based on whether the change magnitude exceeds a specific threshold. The following Fig. 7(a) and (b) shows the results of applying change vector analysis and change detection binary map.

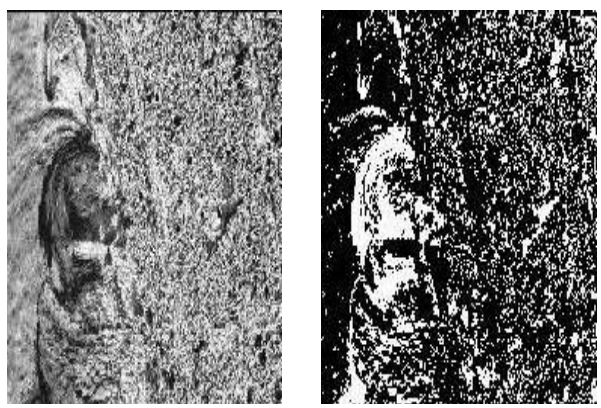

Fig 7. (a) Change Vector Analysis (b) Change Detection

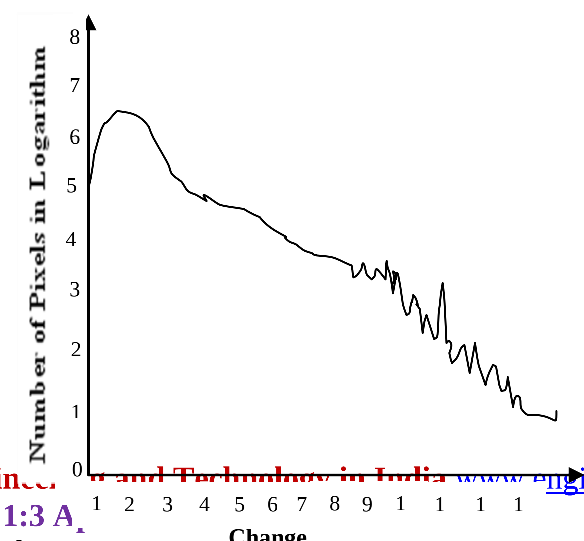

Engineering & Technology in India ISSN 2472-8640

Change magnitudes between two temporal images were calculated and shown in Fig 8. The change magnitudes range from 10 to 130 and most change magnitudes fall under 80. From Fig 8, it is obvious that greater values occur in the north part of the image.

V. CONCLUSION

In this paper, an unsupervised change detection method is proposed and implemented in land use and land cover images. The core idea of the system is to identify the changes between the temporal images. The system extracts the features using UDWT. Feature subset selection is performed by GA. From the selected subset features change map or no change map generation using direct change detection method by CVA.

==

REFERENCES

[1] B. Uma Shankar,Saroj K.Meher, Ashish Ghosh , "Wavelet Fuzzy Hybridization: Feature Extraction and land-cover classification of remote sensing images", Elsevier journal on Applied Soft Computing 11, pp. 999–3011, 2011.

[2] T. Chan and L. Vese, "Active contours without edges," *IEEE Trans. Image Process*., vol. 10, no. 2, Feb. 2001.

[3] Teerasit Kasetkasem and Pramod Kumar Varshney ,"An image change detection algorithm based on Morkov Random Field Models", IEEE Transaction Geoscience Remote Sensing, Vol. 40, No. 8, pp. 1815- 1823, 2002.

[4] T. Celik and K.K. Ma, "Unsupervised change detection for satellite images using dual-tree complex wavelet transform," *IEEE Trans. Geosci. Remote Sens*., vol. 40, no. 8, Aug. 2002.

[5] Turgay Celik "Unsupervised Change Detection in Satellite Images Using Principal Component Analysis and k-means Clustering", IEEE Geoscience Remote Sensing Letter, Vol. 6, No. 4, pp. 772-776, 2009.

[6] Turgay Celik and Kai-Kuang Ma, Senior Member, IEEE "Multitemporal Image Change Detection Using Undecimated Discrete Wavelet Transform and Active Contours", IEEE Transactions on geoscience and remote sensing, Vol. 49, No. 2, pp. 706-716, 2011.

[7] Y. Bazi and F. Melgani, "A Variational level-set method for unsupervised change detection in remote sensing images," in *Proc. IEEE Int. Conf. Geosci. Remote Sens. Symp.*, Jul. 2009, vol.2

==

R. Padmapriya, M.E.
Assistant Professor
Department of ECE
priyasaran600@gmail.com

Dr. V. Ilankumaran
Principal

Renganayagi Varatharaj College of Engineering
Salvarpatti, Thayilpatti
Sivakasi 626128
Virudhunagar District
Tamil Nadu
India

==

Engineering & Technology in India www.engineeringandtechnologyinindia.com
Vol. 1:3 April 2016

==

Amended Golomb Coding (AGC) Implementation for Reconfigurable Devices

Saranya G., M.E.
Loganya R., M.E. Student

==

Abstract

An efficient lossless compression technique to reduce the configuration time of reconfigurable devices known as AGC (AMENDED GOLOMB CODING) is proposed. The time for loading of the configuration data from outside the chip often bottlenecks the system performance for some dynamically reconfigurable applications. Reducing the amount of configuration data with compression technique is one of the efficient approaches to improve the configuration speed. In this paper existing lossless compression technique known as Golomb Codes is amended so that compression efficiency for reconfigurable devices is still enhanced. In AGC the codeword is generated by appending the optimal prefix (amending the original Golomb's prefix), hole bit and tail in such a way that compression efficiency is enhanced.

Key words: AGC, Compression Efficiency, Golomb codes, Lossless compression, optimal prefix.

I. INTRODUCTION

Compression is a way of reducing the original bits required to transfer the source of information while preserving the original content at the decompression side for the purpose of effective transmission and enhancing the storage capacity. Compression reduces the amount of data storage space and data transmission time. Compression is performed by a program that uses a formula or algorithm to determine how to shrink the size of the data. The same program can be used at the receiver side for decompression [4].Text compression can be as simple as removing all unneeded characters, inserting a single repeat character to indicate a string of repeated characters, and substituting a smaller bit string for a frequently occurring bit string. Compression can be performed on the data content or on the entire transmission unit, including header data. Data compression is usually of two types: lossy and lossless [11]. Lossless compression is a class of data compression algorithms that allows the original data to be perfectly reconstructed from the compressed data. Lossless compression algorithms reduce file size with no loss in image quality. The original data is retrieved as it is at the decompression stage. This is because file is only "temporally thrown away" and not discarded hence we could read the original data without loss of information. While the advantage of this is that it maintains quality the main disadvantage is it doesn't reduce the file size as much as lossy compression. Lossy compression permits reconstruction only of an approximation of the original data, though this usually improves compression rates (and therefore reduces file sizes). Lossy compression also looks for 'redundant' pixel information, however, it permanently discards it. This means that when the file is decompressed the original data isn't retrieved. Lossy compression isn't used for data. Lossy is only effective with media elements that can still 'work' without all their original data. The Golomb code can be applied, if numbers of unknown size to be saved, but the actual application is in data compression .Golomb code can similarly efficient as the Huffman code [8] to be, but is more economical in the sense it occupies less memory, and is easier to implement and faster in execution. The proposed AGC is still effective since it enhances the compression achieved by GOLOMB and it could be compared with previous lossless compression [5].

The remainder of this paper is organized as follows. Section II gives a brief review of basic GOLOMB compression. Section III presents proposed AGC and the generation of runlength and codes based on optimal prefix and tail is discussed. In Section IV, programs were executed to verify the validity of our proposed AGC and compared with previous techniques. Finally, conclusions are drawn in Section V.

II. BASIC GOLOMB COMPRESSION

Golomb coding is lossless data compression algorithm [1] .It is a practical and powerful implementation of Run-Length Encoding of binary streams. Golomb coding algorithm contains tunable parameter M, run length N which means count of continuous number of 0"s followed by 1. In Golomb Coding, the group size, *m*, defines the code structure. In order to have simplicity in development and testing, the Golomb coding parameter *m* is set to 4.

Once the parameter *m* is decided, a table which maps the runs of zeros until the code is ended with a one is created [7]. A run length of multiples of *m* are grouped into *Ak* and given the same prefix, which is (*k* – 1) number of ones followed by a zero. The prefix is generated as per unary coding. Unary coding is an entropy encoding that represents a natural number n, with n 0‟s followed by 1 if natural number is non- negative or with (n-1) 0‟s followed by 1 if natural number is strictly positive. In Golomb we get unary code by (*k* – 1) number of ones followed by a zero. A tail is given for each members of the group, which is the binary representation of zero until (*m* – 1). The code word is then produced by combining the prefix and the tail.

III. PROPOSED AMENDED GOLOMB CODING (AGC) COMPRESSION FOR RECONFIGURABLE DEVICES

The proposed AMENDED GOLOMB CODING COMPRESSION makes use of the existing GOLOMB to enhance the compression efficiency still. The first step in AGC is to create a table which maps the runs of zero until the code is ended with one is created. In AGC, the group size, M, defines the code structure. Thus, choosing the m parameter decides variable length code structure which will have direct impact on the compression efficiency [7]. For simplicity M is chosen as 4.Determination of the run length is shown as in Fig.1. A run length of multiples of M are grouped into Ak and given the same prefix as per the algorithm. A tail is given for each members of the group, which is the binary representation of zero until (M – 1). The codeword is then produced by combining the prefix and the tail. AGC will modify the prefix optimally of basic Golomb in such a way that it still enhances compression. Therefore in AGC coding the code word would be generated by joining optimal prefix and tail.

Data	01 0000001 0001 000001 0011					
Subset	01	000000	000	00000	001	1
Run-Length	1	6	3	5	2	0

Fig. 1. Determination of Runlength

Generation of optimal prefix and tail is based on the algorithm given below. The codeword is obtained by joining optimal prefix and tail. Based on the algorithm and M value the code word could be generated. The main advantage of AGC is that we need not to keep track of table or tree as of existing lossless techniques [5].That is it is easier way to implement. The algorithm of AGC is given below:

Golomb coding is implemented using following 3 steps.

1. Fix the parameter M to an integer value.
2. For N, the number to be encoded, find a. quotient = q = int[N/M]

   b. remainder = r = N modulo M
3. Generate Codeword

   a. The Code format :<
   hole bit> <Quotient
   Code>

   <Remainder Code>, where

   b. Quotient Code (optimal group prefix in unary coding)

   i. If 0 □ q □ 1 assign prefix as „q‟.

   ii. If 2 □ q □ 5 assign prefix as binary representation of

   q-2 in 2-bit representation.

   iii.If 6 □ q □13 assign prefix as binary representation of

   q-6 in 3-bit representation and so on..

   c. Remainder Code (in truncated binary encoding) (tail)

   i. If M is power of 2, code remainder as binary format.

   So $\log_2$ (M) bits are needed. (Rice code).

   ii. If M is not a power of 2, set b= [$\log_2$ (M)]

   a .If $r < 2^{b}$-M Code r as plain binary using *b*-1 bits.

   b. If $r > 2^{b}$-M Code the number $r + 2^{b}$-M in plain binary representation using b bits.

Using Fig. 2, binary strings can be divided into subsets of binary strings. Based on the above algorithm and the run Length from Fig.1 optimal prefix and tail is generated. Codeword is generated by appending optimal prefix and tail. In original Golomb prefix generation would be

as follows:

For M and runlength N find quotient q where
$q = \text{int}\,[N/M]$.

In codeword Quotient Code would be: Quotient Code (in unary coding)

i. Write a q-length string of 1 bits ii. Write a 0 bit

In AGC optimal prefix still compresses the bits so that compression is still increased. Substrings are generated by dividing the original strings until 1 is encountered. Binary strings can be divided into subsets of binary strings and replacing the subsets with the equivalent code word as shown in Fig.2.

Group	Run-length	Holebit	Group prefix	Tail	Codeword
A1	0	1	0	00	000
	1	1		01	001
	2	1		10	010
	3	1		11	011
A2	4	1	1	00	100
	5	1		01	101
	6	1		10	110
	7	1		11	111
A3	8	1	00	00	0000
	9	1		01	0001
	10	1		10	0010
	11	1		11	0011
A4	12	1	01	00	0100
	13	1		01	0101
	14	1		10	0110
	15	1		11	0111

Fig. 2. Amended Golomb coding example with parameter M= 4

A hole bit is appended before the optimal prefix which acts as the distinction between the code word which is discarded at the decoder stage. Generation of prefix is stated in state diagram Fig.3.When Runlength is between 0- 3 prefix is generated as „0"and the group is A1.As long as the runlength is 0-3 it remains in the same state A1 and when Runlength 4-7 is encountered it goes to state A2 that is prefix „1"is generated and when Runlength is 8-11 it goes to state A3 and prefix „00" is generated. When Runlength is 12-15 it goes to state A4 and prefix „01"is generated and so on. Whatever may be the present state when runlength changes out of that particular group it changes its state and corresponding optimal prefix is generated.

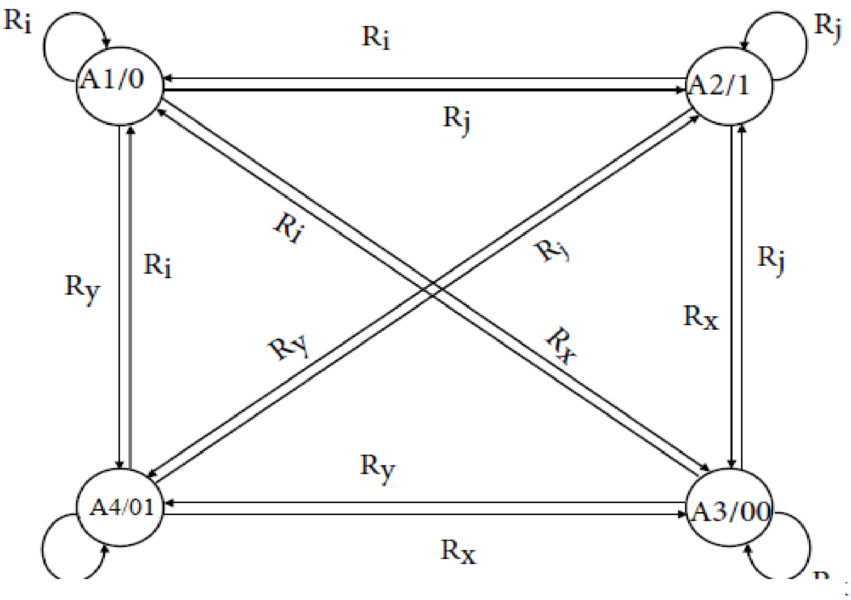

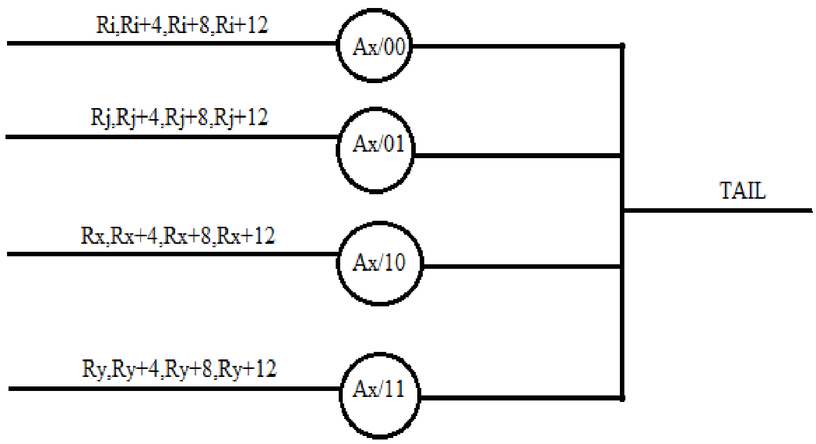

s generated (refer
ıich is the binary
ıced by combining

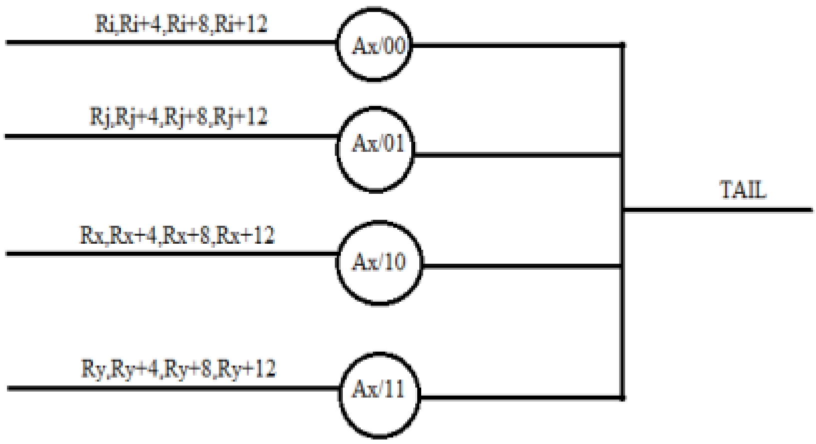

Fig. 4.Tail generation for M=4 (here Ax-Group=1 or 2 or 3 or 4

Ri,Rj,Rx,Ry-Run Length.wherei=0,j=1,x=2,y=3)Whatever may be the group the tail is generated as per the remainder of N/M. In Fig.4 for i, the tail is „00‟ as remainder is 0.For j, the remainder is 1 so the tail is „01‟.As the remainder is 2 the tail is „10‟ for x. For y the tail is„11‟because the remainder is 3.The code word is generated by appending the hole bit, optimal prefix and tail. And at the decompression stage hole bit which act as distinction is now isolated and discarded and the original data is retrieved as it is. Hence become a lossless compression. The proposed AGC still reduces the bits as compared to the existing GOLOMB codes.

IV. RESULTS

The proposed AGC is simulated and compared with expected output and is shown in Fig.5.It is shown that proposed AGC reduces the bits effectively. Compression efficiency is calculated as below:

$$\text{Compression efficiency} = \frac{\text{Uncompressed bits}}{\text{Compressed bits}} * 100$$

INPUT	00010000 00101010 00100000 00000110 00001000 10101011 00010000 01010100 00000001 00010001 00000000 00000001

INPUT SUBSET	**RUN LENGTH**	**EXPECTED AGC OUTPUT**
0001	3	011
0000001	6	1010
01	1	001
01	1	001
0001	3	011

00000000001	10	11010
1	0	000
000001	5	1001
0001	3	011
01	1	001
01	1	001
01	1	001
1	0	000
0001	3	011
000001	5	1001
01	1	001
01	1	001
0000000001	9	11001
0001	3	011
0001	3	011
00000000 00000001	15	0111
OUTPUT	01110100 01001011 11010000 10010110 01001001 00001110 01001001 11001011 0110111	

Fig. 5.Expected output of simulation

The compression efficiency is calculated for the proposed AGC and compared with existing lossless compression techniques Bitmasking (BM), Runlength encoding (RLE) Dictionary (DIC) and old Golomb and is compared in Fig 6. Length before and after compression is indicated as LB and LA respectively.Table1gives the comparison of compression efficiency of various techniques. It is observed that AGC compresses the data more effectively than other techniques.

V.CONCLUSION

In this paper, AGC, An AMENDED GOLOMB CODING (AGC) algorithm a lower complex and less computational load method for data compression and decompression has been proposed.Thus AGC codes are simulated and the result is compared with existing Golomb codes and is proven that Golomb codes are enhanced in the proposed AGC.Amended Golomb coding is highly suitable for situations in which the occurrence of small values in the input stream is significantly more likely than large .

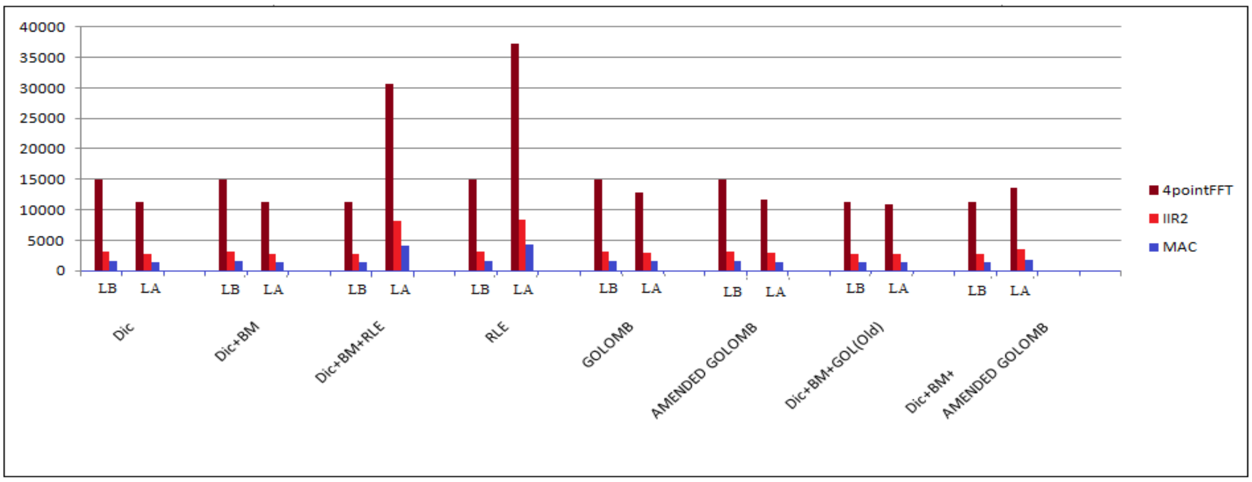

Fig. 6. Comparison of AGC with existing systems

TABLE.1. COMPARISION OF COMPRESSION EFFICIENCY OF VARIOUS TECHNIQUES IN PERCENTAGE

	DIC	DIC+BM	DIC+BM + RLE	RLE	OLD GOLOM B	AMENDE D GOLOMB	DIC+BM + GOL(O L D)	DIC+BM+ AMENDE D GOLOM B
4POINT FFT	1.32	1.33	0.36	0.40	1.17	1.21	1.02	0.82
IIR2	1.16	1.17	0.32	0.36	1.02	1.03	0.95	0.74
MAC	1.06	1.11	0.32	0.33	0.96	1.13	0.95	0.74

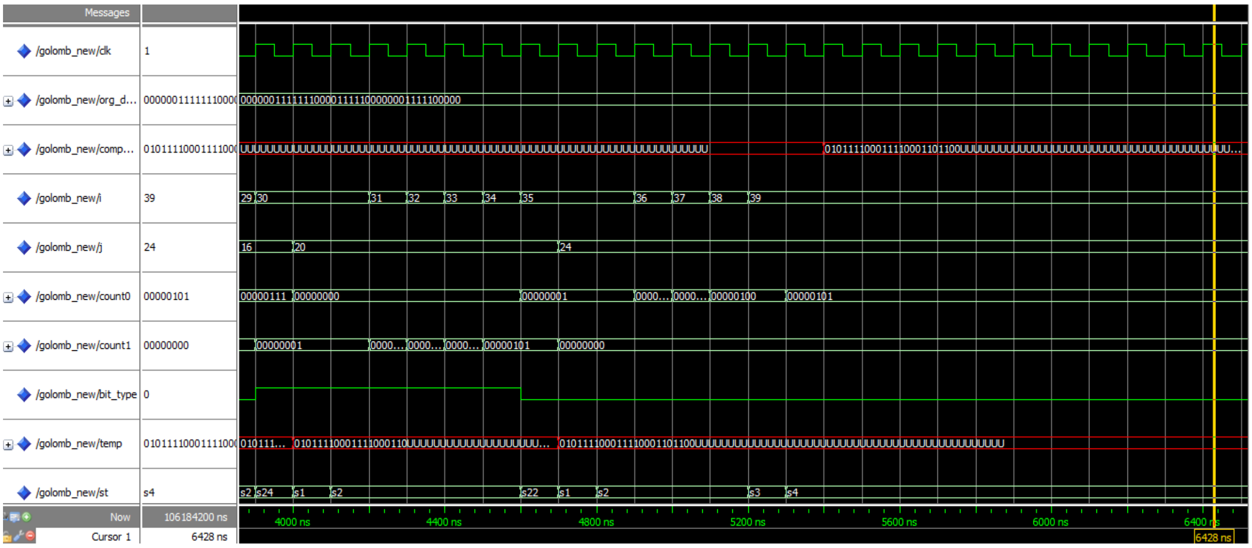

Fig. 7. Simulation output

===

REFERENCES

[1] S. W. Golomb, “Run Length Encodings,” IEEE Transactions on Information Theory, vol. 12, pp. 399-401, 1966.

[2] Chandra and K. Chakrabarty, "System on-a-chip test data compression and decompression architectures based on Golomb codes," IEEE Trans. Computer-Aided Design, vol. 20, pp.355-368, Mar. 2001.

[3] Wang S.J. and Chiou S.N. (2001), „Generating efficient tests for continuous scan", in Proceedings of Design Automation Conference, PP. 162-165.

[4] M. Ghanbari, Video Coding an Introduction to Standard Codecs. London: The Institution of Electrical Engineering, UK, 2003.

[5] T. Sikora, "Trends and perspectives in image and video coding," Proceedings of IEEE, vol. 93, no. 1, pp. 6-17, Jan 2005.

[6] T. Silva, et. al.," FPGA based design of CAVLC and Exp-Golomb coders for H.264/AVC baseline entropy coding," Proc 3rd IEEE Southern Conference on Programmable Logic, pp. 161-166, Feb 2007.

[7] G. H. H"ng, M. F. M. Salleh and Z. A. Halim,"Golomb Coding Implementation in FPGA", Faculty of Electrical Engineering Universiti Teknologi Malaysia VOL. 10, NO. 2, 2008, 36-40.

[8] F. Marcelloni and M. Vecchio. 2009. "An efficient lossless compression algorithm for tiny nodes of monitoring wireless sensor networks," Computer Journal, Vol. 52, No.8, pp.969 – 987.

[9] Tharini and P. Vanaja Ranjan. 2009. "Design of modified adaptive Huffman data compression algorithm for wireless sensor network," Journal of Computer Science, Vol. 5, No. 6, pp. 466– 470.

[10] Ayari, N., LIP2 LabTunis, Tunisia ; Thé Van Luong " hybrid genetic algorithm for Golomb ruler problem",Computer Systems and Applications (AICCSA), 2010 IEEE/ACS International Conference,pp.1 - 4 ,May 2010.

==

Saranya G.
Assistant Professor
Saranyagr80@gmail.com

Loganya R., M.E. Student
Loganya.bharani@gmail.com

Department of Electronics & Communication Engineering
Sri Subramanya College of Engineering & Technology
NH - 209, Sukkamanaickenpatti
Palani 624615
Tamil Nadu
India

==
Engineering & Technology in India www.engineeringandtechnologyinindia.com
Vol. 1:3 April 2016
==

WIRELESS MICROSENSORS CAPSULE SYSTEM

G. Sudhanthira, M.E. (Applied Electronics)
A. Prema, M.E.

==

ABSTRACT

The interface of enabling technology with advanced product design has shown radical development in the field of intelligent sensor-embedded system design. Numerous applications are envisaged exploiting this interconnectivity, particularly, in the field of biomedical applications. A need, for example, that is of growing demand, is in the field of remote health monitoring and control of critically ill patients, with the help of networked sensors. The continuous monitoring of the health of a patient in a hospital, information fusion from multiple sensor-data as well as broadcasting the recorded data on a network for the ease of access to the clinician and implementing the decisions of clinicians through automated drug delivery units could save millions of precious lives in a country with limited medical experts. This project discribes a method for detecting human gastric-motility dysfunction using a wireless electronic capsule. The capsule's main components include three sensors (temperature, pH, and pressure), an Zigbee transceiver, and batteries. The physiological data measured by the wireless capsule within the human gastric system is transmitted to the PC. These data are continuously monitored and recorded for further medical analysis.

1. INTRODUCTION

Gastric motility is the spontaneous peristaltic movements of the stomach that aid in digestion, moving food through the mach and out through the pyloric sphincter into the duodenum. Excess gastric motility causes pain. Below normal motility is common in labor, after general anesthesia, and as side effect of some sedative hypnotics.

In some people, the rate at which their stomach empties its contents into the small intestine is not normal. This can cause feelings of Nausea, Vomiting, Bloating, etc. Few gastric motility disorders: Gastroparesis or delayed gastric emptying, Rapid gastric emptying (dumping syndrome), Idopathic vomiting, Functional dyspepsia and cyclic vomiting syndrome.

The frequency range of the EGG includes bradygastria (0.50-2.50 cpm), normal range (2.50-3.75 cpm), tachygastria (3.75-10.00 cpm), and a respiratory rate of the duodenum (10.00-15.00 cpm). Specifically, the respiratory rate must be identified before analyzing the frequency spectrum of the EGG. If not, the results may be confused with tachygastria. The studies show that patients who have idiopathic gastroparesis (IGP), functional dyspepsia (FD), or delayed gastric emptying always have an abnormal EGG .

At present, EGG cannot diagnose a specific disease, but it provides evidence for stomach motor dysfunction in various pathological conditions. Advances in very large scale integration (VLSI) architecture and system-on-chip (SoC) design have increased scholarly interest in wireless endoscopic capsules. Its major limitations being No means of lumen diameter adaptation and Lack of tissue interaction.

This led to development of the wireless electronic microsensor system in which capsule is a pill-sized sensor that is swallowed and it measures: Temperature, pH, Pressure, How quickly the stomach empties, How quickly the small intestine and colon empty. The capsule transmits these measurements to a receiver and recorder. This test records helps to diagnose conditions including gastroparesis, colonic inertia, rapid gastric emptying and constipation.

2. RELEATED WORK

` In a research paper "Wireless Telemetry for Electronic Pill Technology" Mehmet R. Yuce, Tharaka Dissanayake, Ho Chee Keong under the Australian Research Council (ARC) , research has been dedicated to the development of a high capacity radio system for a small, miniaturized electronic pill device that can be swallowable or implantable in human body in order to detect biological signals or capture images that could eventually be used for diagnostic and therapeutic purposes. In addition to reviewing and discussing the recent attempts in electronic pill technology, a wideband (UWB) telemetry system aimed for the development of an electronic pill is described in the paper.

In a paper “Swallowable-Capsule Technology” by Colm Mc Caffrey, Olivier Chevalerias, Cian O’Mathuna, and Karen Twomey of Tyndall National Research Institute, the idea of exploring the human body captured the imagination was dealt with. This vision is now becoming more achievable with recent advances in electronics, microsystem fabrication, and wireless communications, and a greater understanding of human physiology. Electronic microsystems can now be ingested to explore the gastrointestinal (GI) tract and can transmit the acquired information to a base station In addition to the standard constraints in electronic design, a number of main challenges arise for systems that operate inside the human body.

“Wearable Sensors for Human Activity Monitoring: A Review” by Subhas Chandra Mukhopadhyay deals with the development of Wearable sensors detect abnormal and/or unforeseen situations by monitoring physiological parameters along with other symptoms. Therefore, necessary help can be provided in times of dire need. This paper reviews the latest reported systems on activity monitoring of humans based on wearable sensors and issues to be addressed to tackle the challenges. And reviewed the reported literature on wearable sensors and devices for monitoring human activities as well

3. SYSTEM DESIGN AND ANALYSIS

The overall system architecture under discussion in presented in Fig. and is comprised of the following two functional blocks:

- A central measurement and transmitting unit
- A monitoring and receiving unit

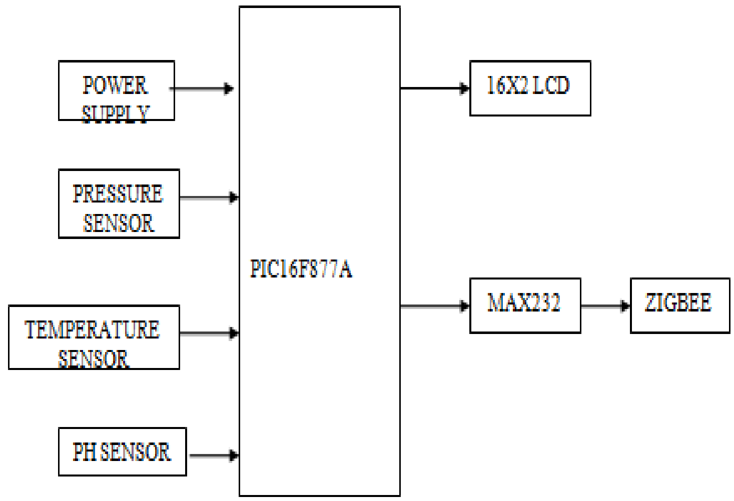

A CENTRAL MEASUREMENT AND TRANSMITTING UNIT

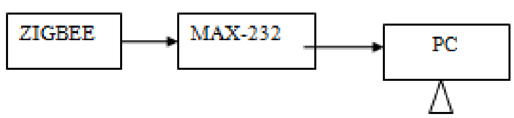

A MONITORING AND RECEIVING UNIT

PRESSURE SENSOR

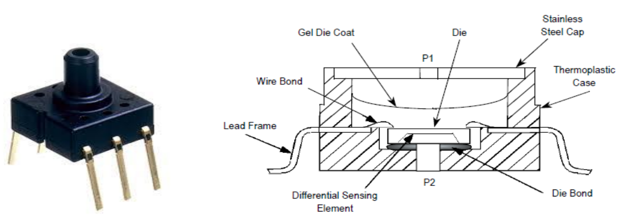

PRESSURE SENSOR

The MPVZ5150 series piezoresistive transducer is a state-of-the-art monolithic silicon pressure sensor designed for a wide range of applications, but particularly those employing a microcontroller or microprocessor with A/D inputs. This patented, single element transducer combines advanced micromachining techniques, thin-film metallization, and bipolar processing to provide an accurate, high level analog output signal that is proportional to the applied pressure.

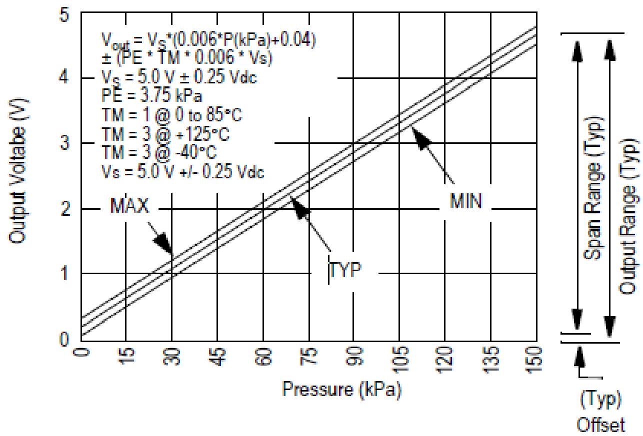

OUTOUT VOLTAGE VS PRESSURE

TEMPERATURE SENSOR

The LM35 series are precision integrated-circuit temperature sensors, whose output voltage is linearly proportional to the Celsius (Centigrade) temperature. The LM35 thus has an advantage over linear temperature sensors calibrated in ° Kelvin, as the user is not required to subtract a large constant voltage from its output to obtain convenient Centigrade scaling. The LM35 does not require any external calibration or trimming to provide typical accuracies of ±1⁄4°C at room temperature and ±3⁄4°C over a full −55 to +150°C temperature range. Low cost is assured by trimming and calibration at the wafer level. The LM35's low output impedance, linear output, and precise inherent calibration make interfacing to readout or control circuitry especially easy. It can be used with single power supplies, or with plus and minus supplies.

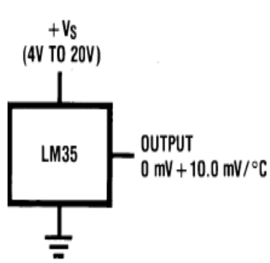

BASIC CENTEGRADE TEMPERATURE SENSOR

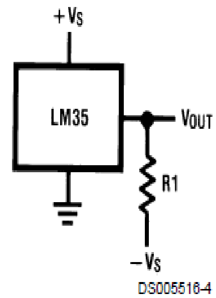

FULL-RANGE CENTEGRADE TEMPERATURE SENSOR

PH SENSOR

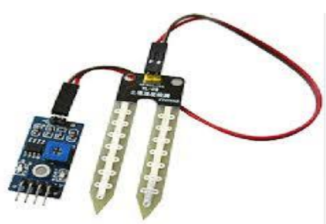

PH SENSOR

pH sensor measures the pH leve.l Basic potentiometric pH meters simply measure the voltage between two electrodes

MICROCONTROLLER - PIC16F877A

The PIC microcontroller [10] is used to interface the energy measurement unit and GSM module. The PIC microcontroller used here is PIC16F877A. .

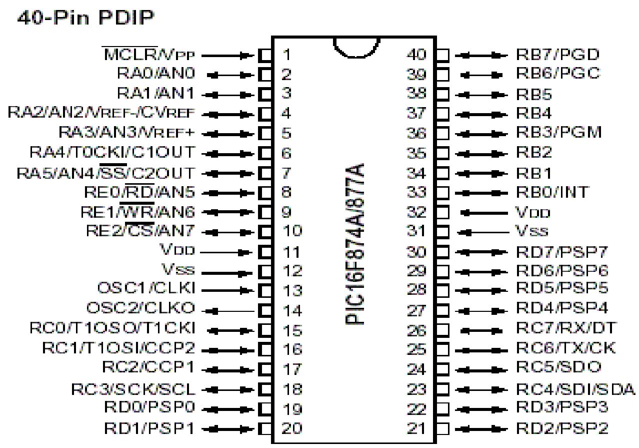

PIN DIAGRAM OF PIC16F87/877A

UNIVERSAL SYNCHRONOUS ASYNCHRONOUS RECEIVER TRANSMITTER (USART)

The USART is two serial I/O modules. The USART can be configured as a full duplex asynchronous system that can communicate with peripheral devices or as a half duplex synchronous system in master or slave mode. Bit SPEN i.e. RCSTA and bit TRISC have to be set in order to configure pins RC6/TX/CK and RC7/RX/DT as the USART. The USART module also has a multi-processor communication capability using 9-bit address detection. The BRG support both the synchronous and asynchronous mode of the USART. It is dedicated 8-bit baud rate generator. The SPBRG register controls the period of a free running 8-bit timer. In asynchronous mode, bit BRGH controls the baud rate. In synchronous mode, bit BRGH is ignored. It is advantageous to use high baud rate for low baud clocks.

USART IN ASYNCHRONOUS MODE

In this mode the USART uses standard Non-return-to zero format. The most common data format is 8-bit. The USART transmits and receives the LSB first. The transmitter and receiver functionality are independent, but use the same data format and baud rate. This mode is selected by clearing bit SYNC (TRISA).

In transmitter the TXREG register is loaded with data. The TSR register is not loaded until the STOP bit has been transmitted from the previous load. As soon as the STOP bit is transmitted, the TSR is loaded with new data from TXREG register. Once the TXREG register transfer the data to the TSR register, the TXREG register is empty and flag bit TXIF is set.

The interrupt can be enabled/ disabled by setting/clearing-enabled bit TXIE. Flag bit TXIF will be set, regardless of the state of enable bit TXIE and cannot be cleared in software. It will reset only when new data is loaded into the TXREG register. While flag bit TXIF indicates the status of the TXREG register, another bit TRMT shows the status of TSR register. The status bit TRMT is read only bit, which is set when the TSR register is empty. Setting enable bit TXEN enables the transmission. The actual transmission will not occur until the TXREG has been loaded with data and the baud rate generator (BRG) has produced a shift clock. First loading the TXREG register then setting enable bit TXEN can also start the transmission.

In reception the data is received on the RC7/RX pin and drives the data recovery block. In the receiver side the data is received serially in shift register. The main block in receiver is receiver shift register (RSR). After sampling the STOP bit, the received data in the RSR is transformed to RCREG register. If the transfer of data is completed, flag bit RCIF is set. The actual interruption can be enabled / disabled by setting/clearing enable bit RCIE. RCIF register is cleared when the RCREG has been read and is empty. RCREG is a double-buffered register. It is possible for two bytes of data to be received and transferred to RCREG FIFO and then shifted to the RSR register. On the detection of the STOP bit, if the RCREG register is still full, the overrun error bit OERR will be set. The word in the RSR will be lost. Overrun bit OERR has to be cleared in the software. This is done by setting the receive logic. If the OERR is set, transfer from the RSR register to the RCREG is inhibited, and no further data will be received. It is essential to clear OERR bit if it is set. Framing error bit is set if a stop bit is detected as a clear. Bit FERR and the 9^{th} receive bit are buffered as the same way as the receive data.

RS 232 COMMUNICATION

To allow compatibly among data communication equipment made by various manufacturers, an interfacing standard called RS232 was set by the Electronics Industries Association (EIA). It was modified and called RS232. It is most widely used for serial I/O interfacing standard. This standard is used for communicating between PIC microcontroller and GSM module. In this standard, a ‘1’ is represented by -3 to -15V, while a ‘0’ bit is +3 to +25V, making -3 to +3 undefined. For this reason, to connect any RS232 to a microcontroller system we must use voltage converter such as MAX 232 to convert the TTL logic levels to the RS232 voltage level, and vice versa.

ZIGBEE TRANSCEIVER

ZigBee and IEEE 802.15.4 are standards-based protocols that provide the network infrastructure required for wireless sensor network applications. 802.15.4 defines the physical and MAC layers, and ZigBee defines the network and application layers.

This is an FSK Transceiver module, which is designed using the Chipcon IC (CC2500). It is a true single-chip transceiver, It is based on 3 wire digital serial interface and an entire Phase-Locked Loop (PLL) for precise local oscillator generation .so the frequency could be setting. It can use in USART / NRZ / Manchester encoding / decoding. It is a high performance and low cost module. It gives 30 meters range with onboard antenna. In a typical system, this trans-receiver will be used together with a microcontroller. It provides extensive hardware support for packet handling, data buffering, burst transmissions, clear channel assessment, link quality indication and wake on radio. It can be used in 2400-2483.5 MHz ISM/SRD band systems. For sensor network applications, key design requirements revolve around long battery life, low cost, small footprint, and mesh networking to support communication between devices in an interoperable environment.

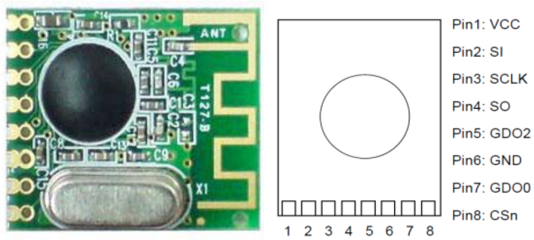

ZIGBEE TRANSIVER BOARD & PIN CONFIGURATION

4. SOFTWARE PLATFORM DESIGN

In our proposed system we have use the Proteus software. Proteus developed by Labcenter Electronics, is a software with which you can easily generate schematic captures, develop PCB and simulate microprocessor. It has such a simple yet effective interface that it simplifies the task required to be performed. It is compatible with both 32 bit and 64 bit systems. Proteus software package splits into three parts very conveniently namely: -

- ISIS Intelligent Schematic Input System - for drawing circuit diagrams etc.
- ARES Advanced Routing and Editing Software - for producing pcb layoutbdrawings.
- LISA Labcenter Integrated Simulation Architecture - for simulation of circuit diagram. Separate handout.

Proteus VSM (Virtual System Modelling) feature allows the real time design simulation. It is armed with the mixed-mode SPICE simulation. The graphical approach also allows non-programmers to build programs by dragging and dropping virtual representations of lab equipment with which they are already familiar. The Proteus programming environment, with the included examples and documentation, makes it simple to create small applications. The back panel contains structures and functions which perform operations on controls and supply data to indicators. The structures and functions are found on the Functions palette and can be placed on the back panel. Collectively controls, indicators, structures and functions will be referred to as nodes. Nodes are connected to one another using wires – e.g. two controls and an indicator can be wired to the addition function so that the indicator displays the sum of the two controls. Thus a virtual instrument can either be run as a program, with the front panel serving as a user interface, or, when dropped as a node onto the block diagram, the front panel defines the inputs and outputs for the node through the connector pane. This implies each VI can be easily tested before being embedded as a subroutine into a larger program.

The graphical approach also allows non-programmers to build programs by dragging and dropping virtual representations of lab equipment with which they are already familiar. The Proteus programming environment, with the included examples and documentation, makes it simple to create small applications.

Features of Proteus:

- Below are some noticeable features.
- Easy to use tool.
- Simple but effective interface.
- Circuit designing and schematic making made easy.
- Provides a powerful working environment.
- Real time design simulation with VSM.
- Can route and edit different components using ARES feature.

Need of Proteus:

Combine the power of Proteus software with modular, reconfigurable hardware to overcome the ever-increasing complexity involved in delivering measurement and control systems on time and under budget.

Application Areas:

- Acquiring Data and Processing Signals
- Automating Test and Validation Systems
- Academic Teaching
- Instrument Control
- Embedded Monitoring and Control Systems

- Wireless System Prototyping

5. SOFTWARE RESULTS

SIMULATED OUTPUT OF THE CAPSULE SYSTEM:

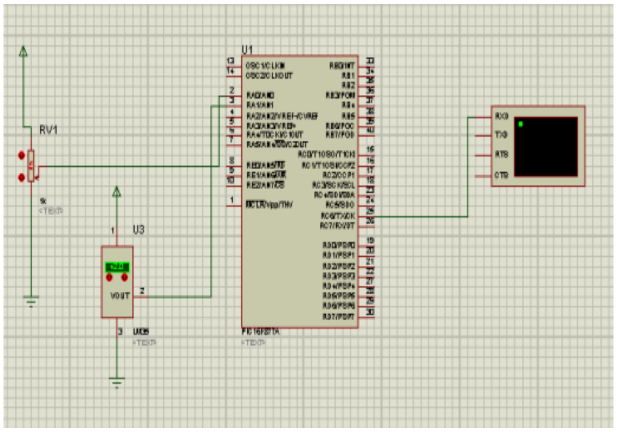

SIMULATED OUTPUT SHOWING VIRTUAL WINDOW:

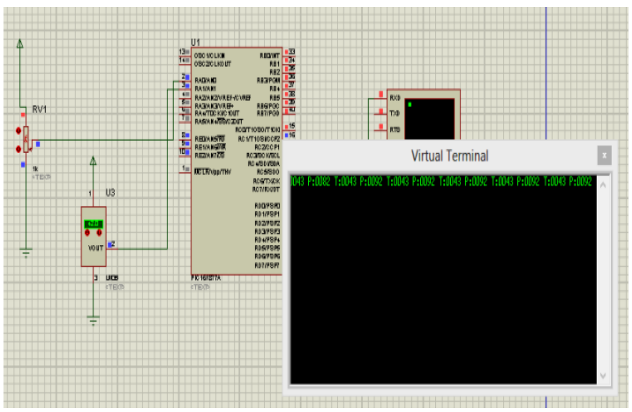

VIRTUAL TERMINAL WINDOW SHOWING VARYING OUTPUTS OF THE SENSORS:

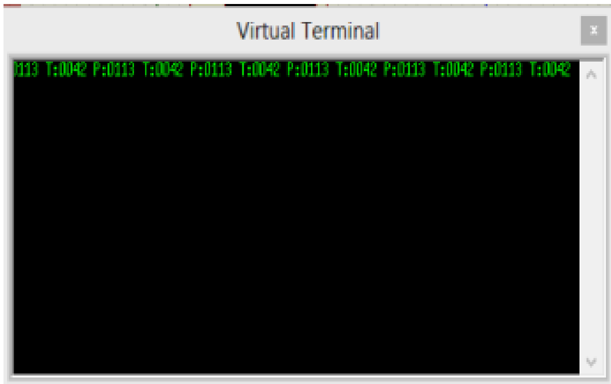

6. Conclusion

Techniques and methodologies have been presented in this project for the use of wideband technology in a miniaturized electronic pill to provide a high capacity wireless channel. Aprototyping system including sensors and transmitter/receiver has been developed to investigate the feasibility of a physiological data transmission for the electronic pill technology.

==

Acknowledgement

We thank the anonymous reviewers for their detailed comments and suggestions, which helped in improving the technical and editorial quality of this paper.

==

REFERENCES

1. Mehmet R. Yuce, Tharaka Dissanayake, Ho Chee Keong under the Australian Research Council (ARC) , "Wireless Telemetry for Electronic Pill Technology"

2. Colm Mc Caffrey, Olivier Chevalerias, Cian O'Mathuna, and Karen Twomey of Tyndall National Research Institute , "Swallowable-Capsule Technology" Published by the IEEE CS 2008

3. Advanced Technologies for Gastrointestinal Endoscopy Pietro Valdastri,1 Massimiliano Simi,2 and Robert J. Webster III314 May 2012

4. Subhas Chandra Mukhopadhyay, "Wearable Sensors for Human Activity Monitoring: A Review" for IEEE Sensors Journal, Vol. 15, No. 3, March 2015

5. Z. D. Goh, P. Georgiou, T. G. Constandinou, T. Prodromakis, and C. Toumazou, "A CMOS-based ISFET chemical imager with autocalibration capability," IEEE Sensors J., vol. 11, no. 12, pp. 3253–3260, Dec. 2011.

6. N. Ollovier-Henry et al., "Design and characteristics of a multichannel front-end ASIC using current-mode CSA for small-animal PET imaging," IEEE Trans. Biomed. Circuits Syst., vol. 5, no. 1, pp. 90–99, Feb. 2011.

7. X. Zhang, H. Jiang, L. Zhang, C. Zhang, Z. Wang, and X. Chen, "An energy-efficient ASIC for wireless body sensor networks in medical applications," IEEE Trans. Biomed. Circuits Syst., vol. 4, no. 1, pp. 11–18, Feb. 2010.

8. L. Wang et al., "A wireless biomedical signal interface system-on-chip for body sensor networks," IEEE Trans. Biomed. Circuits Syst., vol. 4, no. 2, pp. 112–117, Apr. 2010.

9. Varadarajulu S, Banerjee S, Barth BA, Desilets DJ, Kaul V, et al. 2011. GI endoscopes. Gastrointest. Endosc.

10. Rodriguez S, Banerjee S, Desilets D, Diehl DL, Farraye FA, et al. 2010. Ultrathin endoscopes. Gastrointest.Endosc. 71:893–98

11. Gonzalez S, Yu WM, Smith MS, Slack KN, Rotterdam H, et al. 2010. Randomized comparison of 3 different-sized biopsy forceps for quality of sampling in Barrett's esophagus. Gastrointest. Endosc.

12. T. Dissanayake, M. R. Yuce and Ho C. K. "Design and evaluation of a compact antenna for implant-to-air UWB communication," IEEE Antennas and Wireless Prop. Letters, vol. 8, Page(s):153 - 156, 2009.

13. N. Aydin, T. Arslan, and D. R. S. Cumming, "Design and implementation of a spread spectrum based communication system for an ingestible capsule," IEEE Trans. Information Technology in Biomedicine, Vol.9, March 2005.

14. T. Dissanayake, M. R. Yuce and Ho C. K. "Design and evaluation of a compact antenna for implant-to-air UWB communication," *IEEE Antennas and Wireless Prop. Letters*, vol. 8, Page(s):153 - 156, 2009.

==

G. Sudhanthira, M.E (Applied Electronics)
Department of Electronics and Communication
Veerammal College of Engineering
PVP Nagar
Dindigul - Batlagundu Highways
K. Singarakottai
Dindigul 624708
Tamil Nadu
India

A. Prema, M.E. Assistant Professor
Department of Electronics and Communication
Veerammal College of Engineering
PVP Nagar
Dindigul - Batlagundu Highways
K.Singarakottai
Dindigul 624708
Tamil Nadu
India

Vulnerability Level Based Collision Avoidance in Underwater Sensor Networks

V. Anandavenkatesh, II Year M.E (Applied Electronics)
S. Vallimayil, M.E.

==

Abstract

One of the main problems in underwater communication is the low data rate available due to the use of low frequencies. Moreover, there are many problems inherent to the medium such as reflections, refraction, energy dispersion, ect. That greatly degrades communication between devices. In some cases, wireless sensors must be placed quite close to each other in order to take more accurate measurements from the water while having high communication bandwidth. In these cases, while most researchers focus their efforts on increasing the data rate for low frequencies. We show our wireless sensor node deployment and its performance obtained from a real scenario and measures taken for different frequencies, modulations and data transfer rate. The performed test show maximum distance between sensors, the number of lost packets and the average round trip time. We compare our communication system proposal with the existing systems. Although our proposal provides short communication distances, it provides high data transfer rates. It can be used for precision monitoring in application such as contaminated ecosystems or for device communication at high depth.

Keywords: Transmission nodes,Acoustic sensor, Find the shortest path, source and Destination allocation.

INTRODUCTION

An Underwater Sensor Network (UWSN) is an emerging network paradigm which consists of a number of underwater sensor nodes and is deployed to perform collaborative monitoring and resource exploration tasks over a given area [2]. The applications of UWSNs have huge potential for monitoring the health of river and marine environments. Although there are a large number of developed network protocols for wireless sensor networks, the unique characteristics of UWSNs – such as limited bandwidth capacity, large propagation delay and node mobility, as well as high error probability – lead to considerable challenges in their design. This special issue aims to bring together a variety of advanced technologies, theory and applications in the area of UWSNs[4]. We solicit high-quality theoretical as well as practical studies on a broad range of issues important to communications, networks and applications[5].

Ocean bottom sensor nodes can be used for oceanographic data collection, pollution monitoring, offshore exploration and tactical surveillance applications[7]. Moreover, sensors will find application in exploration of natural elements under sea resources and gathering of scientific data in collaborative monitoring missions. Underwater acoustic networking is the enabling technology for these applications[9]. Underwater Networks consist of a variable number of sensors and vehicles that are deployed to perform collaborative monitoring tasks over a given area. In this paper, several fundamental key aspects of underwater acoustic communications are investigated. Different architectures for two-dimensional and three-dimensional underwater sensor networks are discussed, and the underwater channel is characterized[10].

UNDERWATER COMMUNICATION

In this section, we discuss a number of technology issues related to the design analysis, implementation and testing of underwater sensor networks. We begin at the physical layer with the challenges of acoustic communication, then proceed to communications and networking layers, followed by a discussion on applications, hardware platforms, test beds and simulation tools Outside water, the electromagnetic spectrum dominates communication, since radio or optical methods provide long-distance communication (meters to hundreds of kilometers) with high bandwidths (kHz to tens of MHz), even at low power. In contrast, water absorbs and disperses almost all electro- magnetic frequencies, making acoustic waves a preferred choice for underwater Communication beyond tens of meters.

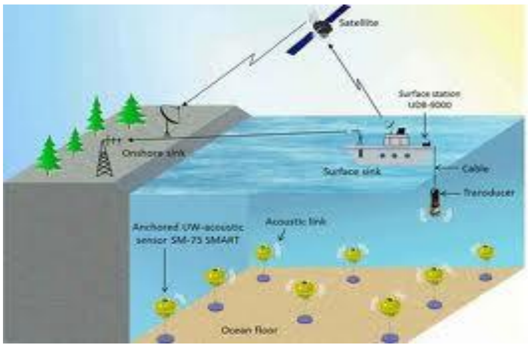

Figure 1. oceanographic system

WIRELESS SENSOR NETWORKS

Using wireless sensor networks for seismic imaging is not a new idea in the sensor network community. But all existing work is based on radio communications among sensors. Our goal is to extend sensor networking technology to underwater applications with acoustic communications. So far, virtually all platforms developed for wireless sensor networks use radio communications. One of most widely vehicles, these approaches can be very inexpensive and in many ways ideal, assuming very high latencies can be tolerated. We see our approach at moderate-distance communication as providing an important complement to data mules. Furthermore, particularly in the case of underwater operation, data mules may benefit from acoustic communication.

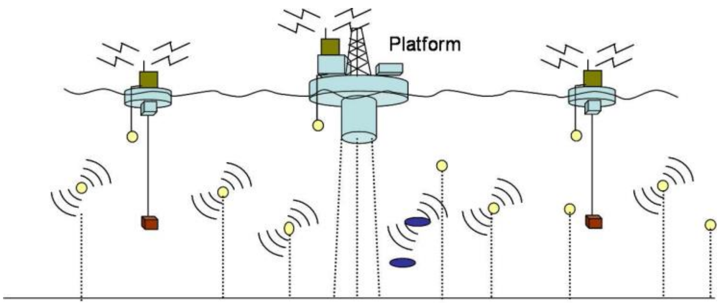

Figure 2. One possible approach to node deployment.

At the top layer are one or more control nodes with connections to the Internet, and possibly human operators. These control nodes may be positioned on an off-shore platform with power, or they may be on-shore; we expect these nodes to have a large storage capacity to buffer data, and access to ample electrical power. Control nodes will communicate with sensor nodes directly, via a relay node: a sensor node with underwater acoustic modems that is connected to the control node with a wired network.

DATA RATE

This is a trade off in the system design, based on available power, and channel bandwidth. Because acoustic communications are possible only over fairly limited bandwidths, we expect a fairly low data rate by comparison to most radios. We see a rate of currently 5kb/s and perhaps up to 20kb/s. Fortunately these rates are within an order of magnitude of RF-based sensor networks. In application such as robotic control, the ability to communicate at all (even at a low rate) is much more important than the ability to send very large amounts of data quickly. In addition, we describe how application-level techniques can be used to maximize the benefits of even limited communications rates. Support for the wired world includes Routing DV, LS, and PIM-SM.and Transport protocols: TCP and UDP for unicast and SRM for multicast. Traffic sources: web, ftp, telnet, cbr (constant bit rate), stochastic, real audio. Different types of Queues: drop-tail, RED, FQ, SFQ, and DRR. Qualities of Service are Integrated Services and Differentiated Services.

MEDIUM ACCESS CONTROL

There has been intensive recent research on MAC protocols for ad hoc and wireless terrestrial sensor networks However, due to the different nature of the underwater environment and applications, there are several drawbacks with respect to the suitability of the existing terrestrial MAC solutions in the underwater environment. In fact, channel access control in UW-ASNs poses additional challenges due to the peculiarities of the underwater channel, in particular limited bandwidth, very high and variable delay, channel asymmetry, and heavy multipath and fading phenomena. Existing MAC solutions are mainly focused on CSMA or CDMA because Frequency Division Multiple Access (FDMA) is not suitable for UW-ASN due to the narrow bandwidth in UW-A channels and the vulnerability of limited band systems to fading and multipath. Moreover, Time Division Multiple Access (TDMA) shows limited bandwidth efficiency because of the long time guards required in the UW-A channel. Furthermore, the variable delay makes it very challenging to realize a precise synchronization, with a common timing reference.

STRUCTURE OF NS2

NS2 is built using object oriented methods in C++ and OTcl (object oriented variant of Tcl.

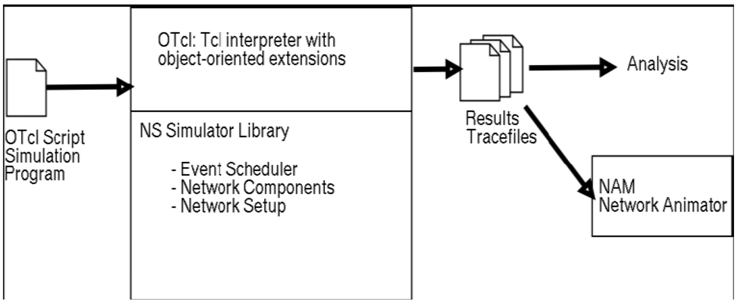

Figure 3. Simplified User's View of Ns

Can see in NS2 interpret the simulation scripts written in OTcl. A user has to set the different components (e.g. event scheduler objects, network components libraries and setup module libraries) up in the simulation environment. The user writes his simulation as a OTcl script, plumbs the network components together to the complete simulation. If he needs new network components, he is free to implement them and to set them up in his simulation as well. The event scheduler as the other major component besides network components triggers the events of the simulation (e.g. sends packets, starts and stops tracing). Some parts of NS2 are written in C++ for efficiency reasons. The data path (written in C++) is separated from the control path (written in OTcl). Data path object are compiled and then made available to the OTcl interpreter through an OTcl linkage (tclcl) which maps methods and member variables of the C++ object to methods and variables of the linked OTcl object. The C++ objects are controlled by OTcl objects. It is possible to add methods and member variables to a C++ linked OTcl object.

This fig.5 represented as schematic entry of six transistors based Static RAM design using S-Edit of TANNER version 13.0 simulator.

NETWORK COMPONENTS

Compound network components shown below a partial OTcl class hierarchy of NS, which will help understanding the basic network components.

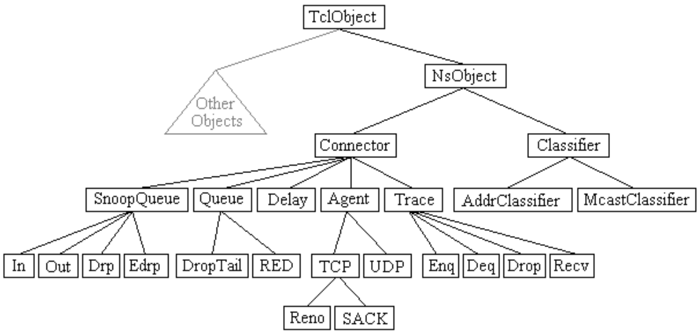

figure 4. Class Hierarchy (Partial)

SENSOR NETWORK INITIALIZED

A group of sensor nodes are anchored to the bottom of the ocean. Underwater sensor nodes are interconnected to one or more underwater gateways (uw-gateways) by means of wireless acoustic links. Uw-gateways are network devices in charge of relaying data from the ocean bottom network to a surface station. To achieve this objective, they are equipped with two acoustic transceivers, namely a vertical and a horizontal transceiver. The horizontal transceiver is used by the uw-gateway to communicate with the sensor nodes in order to: i) send commands and configuration data to the sensors (uw-gateway to sensors); ii) collect monitored data (sensors to uw-gateway). The vertical link is used by the uw-gateways to relay data to a surface station. In deep water applications, vertical transceivers must be long range transceivers.PCAP offers higher throughput than the protocols that are widely used by conventional wireless communication networks. Underwater acoustic sensor networks can be employed by a vast range of applications, retrieving accurate and up to- date information from underneath the water surface. Although widely used by radios in terrestrial sensor networks, radio frequencies do not propagate well underwater.

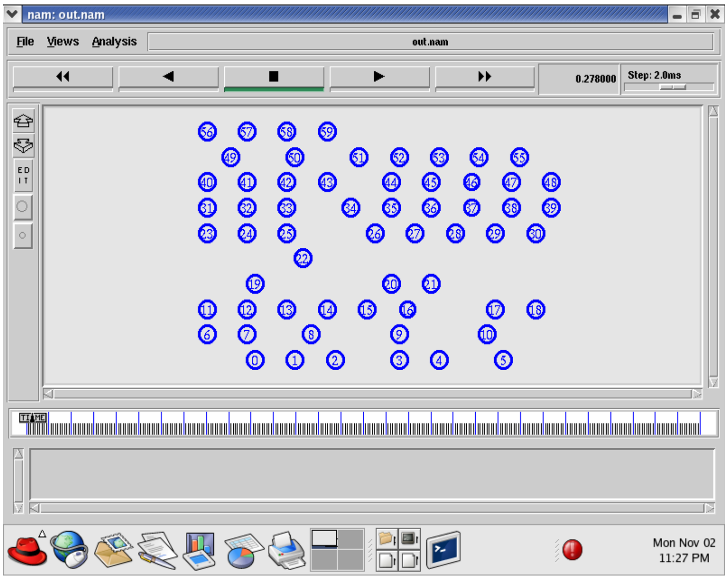

Figure 5. Sensor Network initialized diagram

SENSOR COVERAGE

Since each sensor covers a limited area, adequate coverage of a large area requires appropriate placement of sensors based on collective coverage and cost constraints. The previous research on sensor coverage mainly focuses on studying how to determine the minimum set of sensors for covering every location or certain objects (interest points) in the target field. Different coverage models and methods are surveyed

PROPOSED SYSTEM

The channel capacity, and flow assignment (CCFA) in multi channel wireless mesh networks (WMNs). CCFA involves the joint assignment of channels, distribution of wireless capacity, and determination of link flows to enhance the effectiveness of WMNs. The capacity assignment (CA) problem in WMNs(WMN-CA) which involves the distribution of wireless capacity, given the topology and the flows (i.e., traffic demand and routing).Unlike wired networks, the capacities of different wireless link in a WMN have to be carved out of the capacities of wireless nodes, Since the wireless medium is shared by various wireless nodes, interference between different wireless link constraints the distribution of the wireless capacity available at individual nodes. We formulate WMN-CA as a convex non-linear optimization problem (NLP). that are used to construct the network stack for a mobile node.

The components that are covered briefly are Channel, Network interface, Radio propagation model, MAC protocols, Interface Queue, Link layer and Address resolution protocol model (ARP).

SELECT THE ATTACKER

The attacker is normally unwanted signal from the other sources. The data is transmitted from source to destination through several nodes. Any of the nodes between source and destination can be selected as attacker. Acoustic nodes are used to form source and destination and also a attacker. CSMA method is used to indicate the presents of attacker to the user.

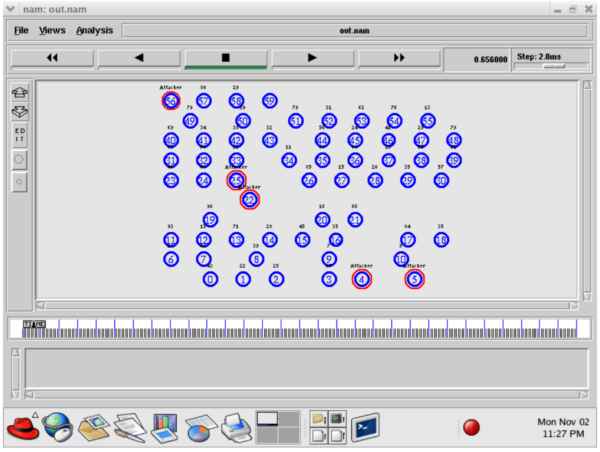

Figure 6. Select the attacker diagram

SOURCE AND DESTINATION

Underwater networks are used to detect and observe phenomena that cannot be adequately observed by means of ocean bottom sensor nodes, i.e., to perform cooperative sampling of the ocean environment. In three-dimensional underwater networks, sensor nodes float at different depths to observe a phenomenon. One possible solution is to attach each uw-sensor node to a surface buoy, by means of wires whose length can be regulated to adjust the depth of each sensor node. However, the floating buoys may obstruct ships navigating on the surface, or they can be easily detected and deactivated by enemies in military settings. Furthermore, floating buoys are vulnerable to weather, tampering, and pilfering. An alternative approach is to anchor sensor devices to the bottom of the ocean. Network Simulator (NS2) is a discrete event driven simulator developed at UC Berkeley. It is part of the VINT project. The goal of NS2 is to support networking research and education. It is suitable for designing new protocols, comparing different protocols and traffic evaluations. NS2 is developed as a collaborative environment. It is distributed freely and open source. A large amount of institutes and people in development and research use, maintain and develop NS2. This increases the confidence in it. Versions are available for FreeBSD, Linux, Solaris, Windows and Mac OS X.

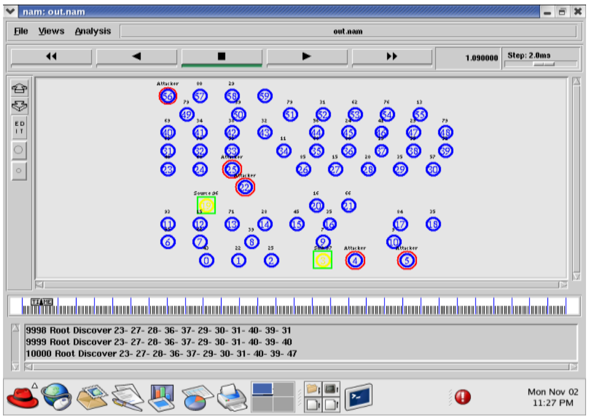

Figure 7. source and destination allocation

DATA TRANSIMISSION

After the initialization phase is complete, each node knows when it needs to wake up again to receive data from its neighbors. After this initialization, nodes follow their established schedules and begin sending data. Fig. 4 shows the structure of the data transmission packet and the listen period to listen to any potential newcomers during the data transmission phase. The transmit duration has been shaded and is followed by a listen duration. The transmit duration has three distinct parts: “missing,”“SYNC,” and “data Tx.” The “data Tx” corresponds to the part where actual data is being sent. We now explain the first two control functions.

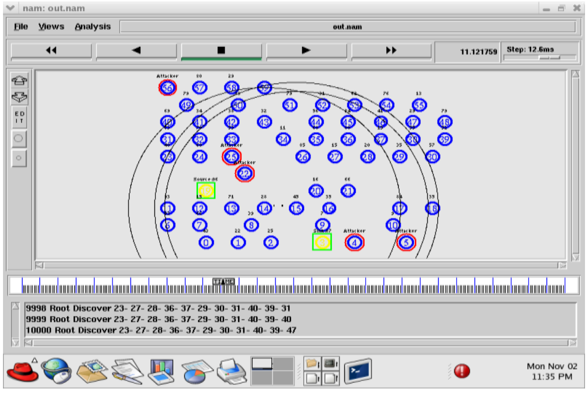

Figure 8. Data transmission

EXISTING SYSTEM

Acoustic channels are therefore employed as an alternative to support long-distance and low-power communication underwater, even though such channels suffer from long propagation delay and very limited bandwidth. In this paper, we investigate the impact of the large propagation delay on the throughput of selected classical MAC protocols and their variants.

RESULT AND DISCUSSION

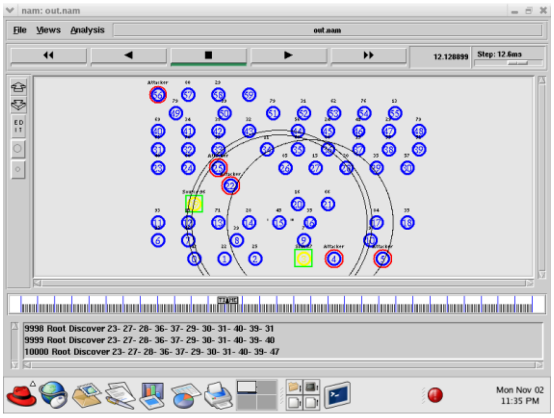

CONCLUSION

We proposed an efficient multichannel Routing protocol for UWSNs in this paper required only one modem for each node utilizing cyclic quorum systems, nodes running MM-MAC are guaranteed to meet their intended receivers, which solves the missing receiver problem. The separations of control and data transmission also help reduce the collision probability of data packets. Simulation result verified that MM-MAC has better performance in that it achieves higher throughput and keeps the retransmission overhead low. We believe that the proposed scheme is a promising multichannel MAC protocol for USWNs since it achieves a great improvement over existing MAC protocol such as slotted FAMA and slotted PCAM.

===

REFERENCES

1. Xiaoxing Guo, Michael R. Frater, Michael J. Ryan, "A Propagation-delay- tolerant Collision Avoidance Protocol for Underwater Acoustic Sensor Networks",1-4244-0138-0/06/$20.00 ©2006 IEEE.

2. Borja Peleato and Milica Stojanovic "A MAC Protocol for AdHocUnderwater Acoustic Sensor Networks",WUWNet'06, September 25, 2006, Los Angeles, California, USA.

3. Dario Pompili,Tommaso Melodia, Ian F. Akyildiz, "A Distributed CDMA Medium Access Control for Underwater Acoustic Sensor Networks", Broadband and Wireles Networking LaboratorySchool of Electrical and Computer Engineering

4. Borja Peleato and Milica Stojanovic, "Distance Aware Collision Avoidance Protocol for Ad-Hoc Underwater Acoustic Sensor Networks", IEEE COMMUNICATIONS LETTERS, VOL. 11, NO. 12, DECEMBER 2007.

5. "Adaptive Routing in Underwater Delay/Disruption Tolerant Sensor Networks", Zheng Guo¤, Gioele Colombi, Computer Science & Engineering Department, University of Connecticut, Storrs, CT, 06269, USA

6. "AN ENHANCED DYNAMIC TOKEN PROTOCOL FOR UNDERWATER ACOUSTIC SENSOR NETWORKS", Guangyu Fan*1, a, Jian Li2, b,Wenhong Liu3, Yang Zhao4, INTERNATIONAL JOURNAL ON SMART SENSING AND INTELLIGENT SYSTEMS,

VOL. 5, NO. 4, DECEMBER 2012

7. “A Receiver-initiated MAC Protocol for Underwater Acoustic Sensor Networks”, Wen-Hwa Liao, 978-1 -4799-3689-2/1 4/$31 .00 ©2014IEEE.

8. 6. Fatemeh Fazel, Milica Stojanovic and Geert Leus, “Packet Scheduling for Underwater Acoustic Sensor Network”, LocalizationHamid Ramezani, IEEE2014

9.Weihong Zhai, Jun Zhang, Sindhu Hak Gupta, “Asynchronous Reservation MAC Protocol for Underwater Acoustic Sensor Network”, 2014 International Conference on Signal Processing and Integrated Networks (SPIN)

10. Hamid Ramezani,StudentMember, IEEE, Fatemeh Fazel, Member, IEEE, Milica Stojanovic, Fellow, IEEE, and Geert Leus, Fellow IEEE, IEEE TRANSACTIONS ON WIRELSS COMMUNICATIONS, “Collision Tolerant and Collision Free Packet Scheduling for Underwater Acoustic Localization”, VOL14, issue 15,may7 ,2015

==

V. Anandavenkatesh
II Year M.E (Applied Electronics)
vanand1893@gmail.com

S. Vallimayil, M.E.
Assistant Professor / Department of ECE

Renganayagi Varatharaj College of Engineering
Salvarpatti
Sivakasi 626128
Tamilnadu
India
vallimayil2009@gmail.com